The Catalan Light Cone:
Dyck Paths as a Discrete Substrate for Causal Geometry, Quantum Amplitudes, and Computation

Paul Fernandez

Abstract

We study the Catalan family of structures—Dyck paths, full binary trees, and balanced parenthesis expressions—as a single discrete space of admissible histories with multiple equivalent "coordinate systems." The Dyck constraint induces a natural causal prefix order, and organizing histories by tier and lateral spread yields a discrete cone whose extremal configurations reproduce a light-cone–like causal envelope.

Classical results on conditioned random walks imply that, under diffusive scaling, Dyck ensembles converge to Brownian excursions. This provides a continuum comparison in which the induced evolution is governed by the heat operator on the half-line (as a base diffusion generator), with the Dyck conditioning encoded via a Doob transform / Bessel-bridge representation, and under analytic continuation one obtains the free Schrödinger equation.

The same Catalan shapes also serve as unlabeled application skeletons for λ-calculus and SKI terms (after choosing a standard finite encoding of symbols). Under this reading, causal extension aligns with functional application while local collapse aligns with computational reduction. We also present a minimal Catalan amplitude model: given an observable/coarse-graining f and a phase functional (e.g. Dyck area), coherent summation over the preimages $f^{-1}(x)$ produces interference under Born-style squaring.

Throughout, we distinguish rigorously established statements (combinatorics, scaling limits, and commutation of disjoint local rewrites) from interpretive or open extensions (measurement, interactions, constants).

1 Introduction

Discrete approaches to fundamental physics suggest that continuum spacetime and quantum dynamics may emerge from deeper combinatorial structure. Examples include causal sets [5], discrete random surfaces and Causal Dynamical Triangulations (CDT) [2, 3], spin networks and loop quantum gravity [15], tensor networks [13], and rewriting systems inspired by λ-calculus and combinatory logic.

Typically, however, these models require multiple independent ingredients: a relation or graph for causal structure, an algebra for computation, and additional rules for quantum propagation. This work explores a more economical possibility: that a *single* recursive structure simultaneously supports all three.

The focus is the *Catalan substrate*, the family of structures counted by the Catalan numbers [16], including Dyck paths, full binary trees, and balanced parenthesis expressions. These objects are usually studied in enumerative combinatorics, probability theory, and theoretical computer science. Here they are treated instead as a space of *admissible histories* generated by a minimal growth constraint.

One object, three coordinate systems. We will move freely between three canonically bijective Catalan families:

- Dyck paths (a constrained nearest-neighbour walk),

- full binary trees (recursive branching structure),

- parenthesis/pairs encodings (a linear trace of the same tree).

Switching between these views is not a simulation; it is a change of representation of the same underlying object. Each view foregrounds different structure: Dyck paths make causal order and scaling limits transparent; trees make locality and computation transparent; and pairs encodings make uniform syntax convenient.

Contributions and scope. The paper isolates a common structural core shared by three domains:

(i) **Causal geometry:** the prefix order on Dyck prefixes induces a discrete causal structure and a cone-shaped envelope with sharp extremals.

(ii) **Continuum comparison:** classical conditioned-walk results yield a diffusion limit (Brownian excursion; the half-line heat operator as a base diffusion generator with the conditioning encoded by a Doob transform), and an analytic-continuation bridge to the free Schrödinger equation [12, 10, 9, 11].

(iii) **Computation:** Catalan tree shapes provide unlabeled application skeletons for standard Turing-complete functional calculi (after choosing a finite encoding of symbols), and local reductions remain internal to the same family [6, 8, 4].

(iv) **Amplitudes:** we define a minimal Catalan amplitude model in which a coarse-graining (observable) and a phase functional determine a coherent sum over indistinguishable histories, producing interference under Born-style squaring.

We do not attempt to derive interactions, constants, or a unique measurement postulate; where additional structure is introduced (e.g. complex phases and Born-style probabilities), it is presented as a minimal construction layered on the Catalan kinematics.

Organization. Section 2 establishes the discrete causal geometry of the Catalan lattice and its interpretation as a light cone. Section 3 develops the computational correspondence via binary application trees and pairs encodings. Section 4 introduces a minimal amplitude construction and the continuum comparison to diffusion and Schrödinger dynamics.[1] Locality and disjoint-commutation are discussed in Section 5. Optional coordinate embeddings, technical notes, and illustrative examples are collected in appendices, separate from the main formal development.

---

[1]Depending on reader background, Sections 3 and Section 4 may be read in either order after the geometric setup in Section 2.

2 The Catalan Light Cone as a Discrete Causal Geometry

2.1 Dyck paths and growth tiers

A Dyck path of semilength n is a walk on the integers satisfying

$$H_{k+1} = H_k \pm 1, \qquad H_k \geq 0, \qquad H_0 = H_{2n} = 0.$$

Equivalently, Dyck paths are balanced parenthesis strings or full binary trees with n internal nodes. The number of such paths is the nth Catalan number

$$C_n = \frac{1}{n+1}\binom{2n}{n}.$$

Each up–down pair () represents a minimal unit of growth. The integer n will be called the *tier* and will be interpreted as a discrete proper time.

2.2 Prefix order and causality

Let $\mathcal{C}$ denote the set of *Dyck prefixes*: balanced-parentheses prefixes that never go below height 0. Define a partial order by extension: $u \preceq v$ iff u is a prefix of v. We interpret this order as a causal relation: $u \preceq v$ means that u lies in the causal past of v, while prefixes that diverge represent incompatible futures. This prefix order defines a discrete causal structure:

- every node has a unique causal past,

- multiple incompatible futures may branch from the same prefix,

- cycles are prohibited by construction.

No additional causal axiom is introduced; causality is enforced combinatorially by the Dyck constraint. Appendix A records an axiomatic characterization of this collision-free two-move growth structure, and Appendix B extends the characterization to growth systems with merges via an explicit unfolding construction.

2.3 Extremal configurations: chain and star

At fixed tier n there are many Dyck paths. Two extremal configurations play a distinguished role:

- the *chain* (or spine)
$$(((\cdots))),$$
fully nested, with maximal depth and minimal spread;

- the *star*
$$()()()\cdots(),$$
fully separated, with minimal depth and maximal spread.

All other configurations interpolate between these extremes. Together, the set of Dyck paths at tier n forms a discrete envelope bounded by the chain and the star.

Remark 2.1 (Narayana refinement by peak count). *In addition to coarse parameters such as depth or breadth, there is a canonical refinement of the tier by the number of* peaks *of a Dyck path (equivalently, the number of occurrences of the pattern ()). The Narayana numbers $N(n,k)$ count Dyck paths of semilength n with exactly k peaks and admit the closed form*

$$N(n,k) = \frac{1}{n}\binom{n}{k}\binom{n}{k-1}, \qquad 1 \le k \le n,$$

with $\sum_{k=1}^{n} N(n,k) = C_n$ [16]. The chain has one peak ($k = 1$) and the star has n peaks ($k = n$). This gives a natural stratification of the tier into k-sectors that interpolate between the two extremes.
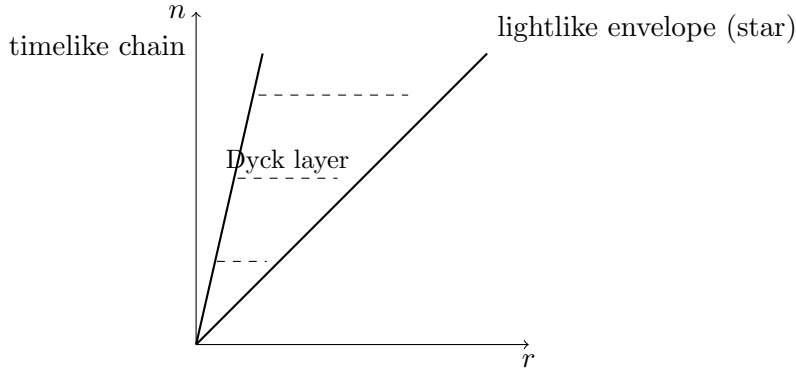

Figure 1: The Catalan light cone. Tier n (the number of Dyck units) plays the role of proper time, while breadth r measures spatial radius. All Dyck configurations at fixed tier lie between the fully nested chain (timelike extreme) and the fully separated star (lightlike envelope). Discrete Dyck layers approximate constant-time hypersurfaces, and the bound $r \le n$ is enforced combinatorially.

2.4   Breadth as spatial extent

Define the *breadth $r(w)$* of a Dyck path w to be the size of a largest level set in the associated full binary tree:

$$r(w) := \max_{\ell}\{\text{number of nodes at depth } \ell\}.$$

Equivalently, $r(w)$ is the maximal number of non-overlapping pairs at a common nesting depth. For a Dyck word of tier n there are n matched pairs in total, so

$$1 \le r(w) \le n,$$

with $r = 1$ for the fully nested chain and $r = n$ for the fully separated star. The inequality

$$r \le n$$

is enforced purely by the recursive constraint. It is the discrete analogue of the relativistic light-cone bound $|\Delta x| \le \Delta t$ (in units with $c = 1$).

4

2.5 Depth–breadth tradeoff

Let $h(w)$ denote the maximum height of a Dyck path, i.e. the maximum nesting depth of its associated full binary tree (root at depth 0). Recall that the breadth $r(w)$ is the maximum number of nodes occurring at any fixed depth level:

$$r(w) := \max_{\ell} \text{ number of nodes at depth } \ell.$$

Depth and breadth are not independent. In any full binary tree, the number of nodes at depth ℓ is at most 2^{ℓ} (each level can at most double from its parent level). Hence, if the maximum level set size $r(w)$ occurs at depth ℓ_*, then

$$r(w) \leq 2^{\ell_*} \leq 2^{h(w)} \quad \Rightarrow \quad h(w) \geq \log_2 r(w).$$

Thus configurations with large breadth necessarily have logarithmically large depth. Equivalently, very shallow trees cannot support wide level sets, while trees with very large depth must concentrate most nodes away from any single breadth-maximizing level.

Remark 2.2 (Kraft equality for leaf depths). *For the full binary tree associated to a Dyck path, if L is the set of leaves and $d(\ell)$ denotes the depth of $\ell \in L$ (root at depth 0), then*

$$\sum_{\ell \in L} 2^{-d(\ell)} = 1.$$

Equivalently, the leaf depths form a complete binary prefix code. This gives a global constraint on allowable depth profiles beyond the crude level bound $r(w) \leq 2^{h(w)}$; see [7].

$$
\begin{array}{ll}
((())) & (h = 3, \ r = 1) \\
(()()) & (h = 2, \ r = 2) \\
(())() & (h = 2, \ r = 2) \\
()(()) & (h = 2, \ r = 2) \\
()()() & (h = 1, \ r = 3)
\end{array}
$$

Figure 2: All Dyck words of tier $n = 3$, ordered from maximal nesting (chain) to maximal separation (star). These five configurations exhaust the discrete causal possibilities at fixed proper time. Depth h and breadth r interpolate between the two extremes, illustrating the intrinsic tradeoff enforced by the Dyck constraint. Higher tiers replicate this structure at larger scale.

2.6 Cone structure

Organizing Dyck paths by tier n and breadth r yields a discrete cone:

- each tier is a "constant-time" slice,
- the chain defines the timelike axis,
- the star defines the lightlike boundary,
- admissible configurations fill the interior.

This structure will be referred to as the *Catalan light cone*.

5

2.7 Scaling behavior

Classical results on conditioned random walks show that typical Dyck paths at tier n have height and breadth of order $\sqrt{n}$ [12, 10, 1]. Extremal configurations saturate the linear bound $r \leq n$, while typical configurations lie deep within the cone. This separation between extremal and typical behavior mirrors the role of null, timelike, and spacelike trajectories in relativistic geometry.

Theorem 2.1 (Discrete light-cone bound and scaling). *Let w be a Dyck word of semilength n and breadth $r(w)$ as above. Then*
$$1 \leq r(w) \leq n.$$

Moreover, for a uniformly random Dyck word of semilength n, the typical height and breadth are of order $\sqrt{n}$.

The first statement follows from the definition of $r(w)$ and the fact that there are n internal nodes, while the scaling behavior is a consequence of invariance-principle results for conditioned random walks [12, 10, 1].

Coordinate charts and continuum comparisons. Appendix C collects optional coordinate-chart constructions (null-count embeddings and related continuum comparisons) used for intuition; the combinatorial results below do not depend on these embeddings.

2.8 Recursive Self-Similarity and Local Re-Centering

A key structural property of the Catalan substrate is its *recursive self-similarity*. Every Dyck word may be viewed as a node in the infinite prefix tree of admissible Dyck prefixes. At any such node u, with current height h and remaining length budget sufficient to return to height 0, the set of all admissible continuations of u forms a subtree whose shape is determined entirely by h. This subtree is canonically isomorphic to the Dyck-prefix tree that begins at height h rather than at height 0.

Formally, let $\mathcal{C}$ denote the Dyck-prefix tree (the poset of Dyck prefixes under extension) and $\mathcal{C}_h$ denotes the Dyck-prefix tree conditioned to start at height h (i.e. with $H_0 = h$ and $H_k \geq 0$ for all k), then for every prefix u of height h we have a canonical isomorphism

$$\mathcal{C}(u) \cong \mathcal{C}_h.$$

In particular, for fixed remaining length, the number of completions depends only on the current height.

Lemma 2.1 (Ballot-number completion count). *Let u be a Dyck prefix of length k with height $h \geq 0$, and fix a target semilength n with $2n \geq k$ for which u admits at least one completion (equivalently $h \leq 2n - k$). Let $r := 2n - k$ be the remaining number of steps. Then the number of Dyck words $w \in \mathcal{D}_n$ having prefix u is*

$$\#\{w \in \mathcal{D}_n : u \preceq w\} = \binom{r}{\frac{r-h}{2}} - \binom{r}{\frac{r-h}{2} - 1} = \frac{h+1}{\frac{r+h}{2} + 1} \binom{r}{\frac{r-h}{2}}.$$

For $h = 0$ (i.e. u is itself a Dyck prefix rooted at the axis), this reduces to the Catalan number $C_{n-k/2}$.

Proof sketch. The completion corresponds to a length-r path of ± 1 steps starting at height h and ending at 0 while staying nonnegative. Writing $r = 2m + h$ (so $m = (r - h)/2$), there are $\binom{r}{m}$ unconstrained sequences with m up steps and $m + h$ down steps. By the reflection principle / Bertrand ballot theorem, the sequences that ever hit -1 are counted by $\binom{r}{m-1}$, so the nonnegative ones are $\binom{r}{m} - \binom{r}{m-1}$, which yields the stated forms; see [16]. $\qquad\square$

Lemma 2.2 (Future cones classified by height). *Let $u, v \in \mathcal{C}$ be Dyck prefixes with heights $h(u), h(v)$. Regard the future cones $\mathcal{C}(u)$ and $\mathcal{C}(v)$ as rooted directed graphs whose edges are the admissible one-step extensions labeled by ((up) and) (down). Then $\mathcal{C}(u)$ and $\mathcal{C}(v)$ are isomorphic as rooted edge-labeled directed graphs if and only if $h(u) = h(v)$. In that case, the canonical isomorphism maps each extension sequence of parentheses appended to u to the same extension sequence appended to v.*

Proof sketch. If $h(u) = h(v) = h$, then admissibility of an extension depends only on the running height above 0, so an extension word s is admissible after u if and only if it is admissible after v. Mapping $us \mapsto vs$ is therefore a bijection on nodes that preserves the labeled extension edges.

Conversely, in $\mathcal{C}(u)$ a node has no)-successor if and only if its height is 0. Starting from height $h(u)$, the minimal directed distance from the root u to such a boundary node is exactly $h(u)$ (follow $h(u)$ consecutive) moves). This distance is an invariant of rooted edge-labeled graph isomorphism, hence $h(u) = h(v)$ whenever $\mathcal{C}(u) \cong \mathcal{C}(v)$. $\qquad\square$

Thus every node of the global Catalan possibility tree is the root of a scaled copy of the entire admissible-future structure, with scaling determined solely by local height. The recursive decomposition of full binary trees,

$$T = \bullet(T_L, T_R),$$

makes the same fact explicit in the tree representation: each subtree of a Catalan tree is itself a Catalan tree, and the decomposition applies inductively at every depth.

This recursive self-similarity has two important consequences for the geometric interpretation developed in this paper:

(i) **Locality and re-centering.** Because the admissible future of any prefix depends only on its present height, not on its global position, the Catalan light-cone geometry is *locally homogeneous*. The causal cone may be re-centered at any node without altering its shape: moving the focus does not change the structure of admissible futures, only the value of the local height at which the cone is rooted.

(ii) **Scale invariance of the substrate.** The same recursive rules govern growth at every depth. The local possibility space looks the same at all scales, in the sense that the subtree below any node is again Catalan. This is the combinatorial source of the invariance principles (Dyck $\to$ Brownian excursion) appearing in the continuum limit.

In summary, the Catalan substrate is self-similar at every node: each point in the possibility space contains a full Catalan future scaled by its current height. This allows the causal and geometric analysis of later sections to be performed relative to *any* node of the prefix tree. The light cone is not anchored to a global origin; it is an intrinsic, relocatable geometric feature of the recursive structure itself.

2.9 Multiple Local Cones and Relational Geometry

The same prefix order that defines causality also yields a family of *local cones*: every Dyck prefix $u \in \mathcal{C}$ induces a future $\mathcal{C}(u)$ of admissible extensions, i.e. the same growth law re-centered at u. Two prefixes u and v relate in exactly two ways:

(i) **Nested cones.** If $u \preceq v$, then $\mathcal{C}(v) \subseteq \mathcal{C}(u)$.

(ii) **Divergent cones.** If neither prefix contains the other, then u and v share a maximal common prefix w and have disjoint futures beyond w.

    Thus the cone picture is relocatable: it appears at every node, cones nest along causal chains, and branching produces incompatible futures.
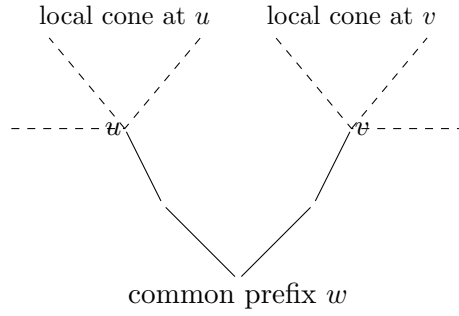

Figure 3: Two Dyck prefixes u and v diverging from a shared ancestor w. Dashed regions indicate the local Catalan cones rooted at u and v. Cones nest along causal chains and diverge after branching points, producing a family of local, relocatable causal geometries on the Catalan substrate.

2.10 Summary

The Catalan substrate supports a discrete causal geometry determined entirely by recursive constraint. Without introducing a manifold, metric, or causal relation by fiat, it yields:

- a partial order interpretable as causality,

- a cone-shaped causal envelope,

- intrinsic bounds on spatial extension,

- well-defined constant-time layers.

Subsequent sections place dynamical rules—computational reduction and a minimal amplitude calculus—on this geometry.

3 Recursive Pairing and Universal Computation

We now read the same Catalan objects from the computational side. Full binary trees serve as application frames, while pairs encodings provide a uniform parenthesis-only syntax. The only additional choice needed to represent concrete programs is an encoding of symbols at leaves.

3.1 Pairs expansion

Catalan shapes as program frames. The Catalan family—Dyck paths, full binary trees, and balanced-parenthesis expressions—forms the free magma on a single binary constructor: it is the space of all finite binary application frames. As observed in classical treatments of the λ-calculus and combinatory logic [8, 4], application is binary, so every SKI term (and every λ-term after fixing a binding convention) has a canonical representation as a finite binary application tree: internal nodes encode application; leaves encode atomic symbols (variables, constants, or combinators). Conversely, any finite binary tree equipped with leaf labels denotes a unique applicative term over that alphabet, modulo surface syntax. Since SKI is computationally universal, this yields an explicit embedding of all computable programs (as terms) within the Catalan substrate. The apparent choice of leaf alphabet can itself be internalized by representing symbols as distinguished Catalan motifs (Remark 3.1).

Remark 3.1 (Symbols as Distinguished Motifs). *Although we sometimes describe leaf labels as an external choice, one may work in a purely structural setting: there is an injective encoding of labeled application trees (and in particular SKI terms) into unlabeled Catalan trees by tagging constructor nodes and representing each symbol by a fixed subtree motif. See Lemma F.1 in Appendix F.*

This observation also extends to operational semantics. Standard reductions (such as β-reduction or SKI contraction) are local rewrite rules on binary trees, and the pairs-expansions of combinators remain within the Catalan family. Accordingly, a program, its intermediate expansion frames, and each permissible reduction schedule are all representable as paths through a single Catalan substrate. Selecting a program shape or selecting a specific reduction history is therefore equivalent to selecting a path in the Catalan tree. In this sense the Catalan substrate uniformly encodes program syntax, program semantics, and the full ensemble of admissible computational histories.

Proposition 3.1 (Catalan Universality for Program Structure). *Let $\mathcal{C}$ denote the Catalan family of finite full binary trees. Every program in any Turing-complete functional calculus (such as the λ-calculus or SKI) admits a canonical representation as an element of $\mathcal{C}$ with leaf labels drawn from a finite alphabet (after fixing a standard encoding of symbols). Conversely, every labeled element of $\mathcal{C}$ denotes a unique program modulo surface syntax. Furthermore, standard operational semantics (including β-reduction and SKI contraction) act as local rewrite rules that preserve membership in $\mathcal{C}$. Thus a program, its syntactic expansions, and every admissible reduction history correspond to paths within the Catalan substrate.*

A proof sketch is provided in Appendix F.

Two canonical parenthesis encodings. There are (at least) two particularly useful parenthesis-only encodings of a full binary tree:

- **Dyck encoding** ("walk" view): balanced parentheses of length $2n$, naturally adapted to height profiles and scaling limits.

- **Pairs (S-expression) encoding** ("cons" view): write each leaf as () and each internal node as a parenthesized pair of its two children, i.e. $T = (L, R) \mapsto (\texttt{enc}(L)\,\texttt{enc}(R))$. This is a variable- and label-free Lisp-style representation with () as the only atom.

In particular, in the *pairs* encoding, the smallest object is the empty pair (), and the smallest nontrivial *binary* object is (()()), i.e. a root pair whose two children are leaves. In the Dyck

encoding, the semilength-1 object is (), since Dyck words begin only after the first matched pair exists.

Handedness and path selection. The Dyck constraint (including return to height 0 at completion) is a well-bracketing discipline: it constrains which histories are admissible, but it does not by itself impose a within-tier ordering of alternatives or select a dynamic among them. By contrast, the applicative reading of Catalan trees as programs requires that internal nodes represent *ordered* pairs (function, argument), i.e. one must fix a convention (e.g. "left applies to right"). This handedness determines syntax, but not which computational history is realized among many permissible ones: selecting a computation corresponds to choosing a reduction strategy (or, in a stochastic formulation, a transition kernel) on the same Catalan substrate.

3.2 A small tier shown three ways (Dyck / tree / pairs)

Figure 4 augments the standard Dyck-$n = 3$ list by displaying, for the *same* five Catalan shapes, the corresponding pairs (S-expression) encodings. For concreteness, the five shapes are listed left-to-right in lexicographic order on Dyck words (with ($<$)), and the tree and pairs rows are obtained by the standard bijection.

$$((()))$$
$$(((()())()())$$

$$(()())$$
$$(((()(()))()))$$

$$(())()$$
$$(((()())(()()))$$

$$()(())$$
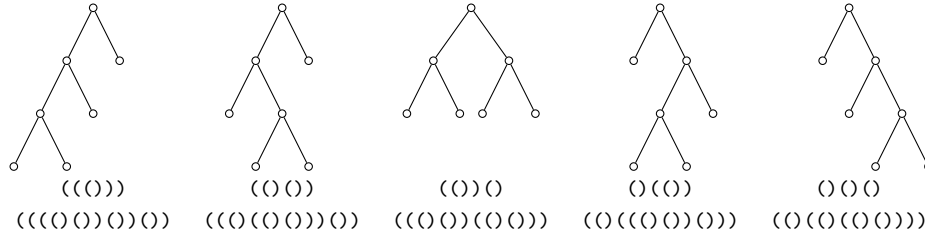$$(()(((()()))()))$$

$$()()()$$
$$(()(()(()())))$$

Figure 4: The five Catalan shapes at tier $n = 3$ shown as (i) full binary trees, together with (ii) Dyck words and (iii) pairs (S-expression) encodings in which each leaf is () and each internal node is a parenthesized pair of its two children (as if one were looking "down into" the tree). These are three coordinate systems for the same underlying Catalan objects.

3.3 Connection to λ-calculus and SKI

Full binary trees are a standard representation of SKI terms, and they capture the application skeleton of λ-terms [6, 8, 4]. A full λ-encoding requires a binding convention (e.g. variables as leaf labels or positions, and abstraction as a structural marker), while application is encoded by the tree's binary node. Under the pairs expansion, each Dyck tree canonically determines an unlabeled application graph. When variables are suppressed, the resulting graphs coincide with the structure graphs used in combinatory logic. No additional primitives beyond recursive pairing are required to obtain this representation.

Choosing a finite set of tree patterns to represent the SKI combinators and interpreting local tree rewrites as SKI reduction therefore equips the Catalan substrate with a standard universal calculus: every partial recursive function can be encoded as an SKI term [8, 4], and hence by a finite Dyck tree, and every computation corresponds to a sequence of local tree transformations. In this sense, the Catalan substrate is *computationally universal*. What is new here is that the same underlying objects simultaneously carry a causal and geometric interpretation.

3.4 Reduction and local collapse

In the computational interpretation, reduction corresponds to local pattern replacement. A redex occupies a finite region of a tree and may be reduced without reference to distant subtrees. This locality mirrors the causal structure established in Section 2. From the perspective of the Catalan lattice, reduction may be viewed as *collapse*: a locally ambiguous structure is replaced by a simpler one consistent with the global constraint. Importantly, collapse does not alter causal ancestry; it refines an already-admissible history. For standard calculi (e.g. λ/SKI), confluence ensures uniqueness of normal forms when they exist, and more locally reductions supported on disjoint subtrees commute [4]. This computational fact will later support an interpretation of spacelike commutativity.

3.5 Summary

Recursive pairing suffices to encode universal computation. Via the pairs expansion, Dyck trees and application graphs are two views of the same structure. Local computational reduction aligns naturally with causal locality on the Catalan light cone.

4 Quantum Amplitudes on the Catalan Lattice

This section layers a minimal amplitude calculus on the Catalan history space. The key inputs are (i) a coarse-graining/observable f identifying which histories are regarded as the same outcome, and (ii) a choice of additive phase functional on histories. Given these, we define amplitudes by coherent summation over preimages and probabilities by normalized squared magnitudes, in analogy with the Born rule [9].

Definition 4.1 (Catalan amplitude model at fixed tier). *Fix a tier n and an observable (coarse-graining) $f : \mathcal{D}_n \to \mathcal{X}$ to a finite outcome set $\mathcal{X}$. Fix a real phase functional $\Phi : \mathcal{D}_n \to \mathbb{R}$, a scale $\alpha \in \mathbb{R}$, and (optionally) a magnitude function $\rho : \mathcal{D}_n \to \mathbb{R}_{\geq 0}$. Define per-history amplitudes*

$$\psi(w) := \rho(w)\, e^{i\alpha\Phi(w)} \in \mathbb{C},$$

where the minimal unit-modulus case is $\rho \equiv 1$. The outcome amplitude and normalized probability are

$$\Psi(x) := \sum_{w:\, f(w)=x} \psi(w), \qquad P(x) := \frac{|\Psi(x)|^2}{\sum_{x' \in \mathcal{X}} |\Psi(x')|^2},$$

whenever the denominator is nonzero.

In what follows we specialize Definition 4.1 to unit magnitude $\rho \equiv 1$ and emphasize additive phase functionals, with the Dyck area $A(w)$ as the main example.

4.1 Histories as paths

Interpreting Dyck paths as admissible histories motivates assigning weights to each history. Let $\mathcal{D}_n$ denote the set of Dyck paths of tier n. A state at tier n may be represented as a formal superposition of histories

$$\Psi_n = \sum_{w \in \mathcal{D}_n} \psi(w)\, |w\rangle.$$

Local extensions of a Dyck path correspond to admissible future steps. Thus, time evolution is governed by transitions that respect the Dyck constraint.

4.2 Observables, projection, and coherent summation

Fix a tier n and consider the set $\mathcal{D}_n$ of Dyck paths of semilength n. Each $w \in \mathcal{D}_n$ represents a complete admissible history at discrete time n, with an associated height profile

$$H_w : \{0, 1, \ldots, 2n\} \to \mathbb{Z}_{\geq 0}.$$

An observable is defined as a deterministic coarse-graining

$$f : \mathcal{D}_n \to \mathcal{X},$$

where $\mathcal{X}$ is a discrete set of outcomes corresponding to a chosen equivalence relation on histories. An outcome $x \in \mathcal{X}$ corresponds to the equivalence class $f^{-1}(x) \subset \mathcal{D}_n$ of histories. By construction, such a projection discards information: many distinct histories may be identified as the same observable outcome.

With no additional structure imposed, the natural measure on $\mathcal{D}_n$ is uniform counting. The induced distribution on the outcome space $\mathcal{X}$ is therefore the pushforward of the uniform counting measure,

$$N(x) := \#\{w \in \mathcal{D}_n : f(w) = x\}.$$

Remark 4.1 (Coherent vs. counting aggregation). *In the uniform counting baseline, the probability of an outcome is proportional to $N(x)$. In the Catalan amplitude model (Definition 4.1) with unit magnitude $\rho \equiv 1$, if the phase functional factors through the observable (i.e. $\Phi = \widetilde{\Phi} \circ f$, so all histories in $f^{-1}(x)$ have the same phase), then*

$$\Psi(x) = e^{i\alpha\widetilde{\Phi}(x)} N(x) \qquad \Rightarrow \qquad P(x) \propto N(x)^2.$$

Destructive/constructive interference occurs only when Φ varies within the fibers $f^{-1}(x)$.

At the opposite extreme, if one models the phases within each fiber as independent uniform random variables (a purely mathematical phase-scrambling toy model), then the unnormalized weights revert to multiplicity in expectation: writing $\Psi(x) = \sum_{j=1}^{N(x)} e^{i\Theta_j}$ with $\Theta_j \overset{\text{iid}}{\sim} \text{Unif}[0, 2\pi)$, one has

$$\mathbb{E}\big[|\Psi(x)|^2\big] = N(x),$$

since the cross terms average to 0 by independence and rotational symmetry.

Even with uniform weight on histories, the induced distribution on $\mathcal{X}$ is generically non-uniform, reflecting the combinatorial geometry of the projection rather than any imposed dynamics.

A discrete analogue of an integral along a history is given by the step-sum of the height profile,

$$A(w) := \sum_{k=0}^{2n-1} H_w(k),$$

which measures the cumulative dwell time at nonzero height. This quantity depends on the full distribution of height along the path, not merely on extrema such as maximum height or peak count.

Remark 4.2 (Area refinement and q-Catalan weights). *Under the standard identification of Dyck paths with lattice paths from $(0, 0)$ to (n, n) staying above the diagonal, the usual* area *statistic* $\text{area}(w)$ *(counting unit squares between the path and the diagonal) satisfies* $\text{area}(w) = (A(w) - n)/2$,

i.e. $A(w) = n + 2\operatorname{area}(w)$. *Consequently, the weighted sum of the area phase is a specialization of the area-refined Catalan generating function:*

$$\sum_{w \in \mathcal{D}_n} e^{i\alpha A(w)} = e^{i\alpha n} \sum_{w \in \mathcal{D}_n} \left(e^{2i\alpha}\right)^{\operatorname{area}(w)}.$$

In particular, any analytic information about the distribution of Dyck area and its generating functions may be transferred directly to these phase-weighted sums [16, 10].

Definition 4.2 (Area-weighted nonnegative bridge kernel). *Fix $\alpha \in \mathbb{R}$. For $r \geq 0$ and $a, b \in \mathbb{Z}_{\geq 0}$, define $K_\alpha^{(r)}(a, b)$ to be the complex weight-sum over all length-r ± 1 paths $(h_0, \ldots, h_r)$ such that $h_0 = a$, $h_r = b$, $h_t \geq 0$ for all t, and $h_{t+1} - h_t \in \{\pm 1\}$, with weight*

$$\exp\left(i\alpha \sum_{t=0}^{r-1} h_t\right).$$

Lemma 4.1 (Transfer recursion and composition for the area phase). *The kernels $K_\alpha^{(r)}$ satisfy:*

(i) **Initial condition:** $K_\alpha^{(0)}(a, b) = \mathbf{1}_{\{a=b\}}$.

(ii) **One-step recursion:** *for $r \geq 0$ and $a, b \geq 0$,*

$$K_\alpha^{(r+1)}(a, b) = e^{i\alpha a}\left(K_\alpha^{(r)}(a+1, b) + K_\alpha^{(r)}(a-1, b)\right),$$

with the convention $K_\alpha^{(r)}(-1, b) = 0$.

(iii) **Chapman–Kolmogorov (semigroup) property:** *for $r, s \geq 0$ and $a, c \geq 0$,*

$$K_\alpha^{(r+s)}(a, c) = \sum_{b \geq 0} K_\alpha^{(r)}(a, b)\, K_\alpha^{(s)}(b, c).$$

In particular, the area-phase partition function at tier n is

$$Z_n(\alpha) := \sum_{w \in \mathcal{D}_n} e^{i\alpha A(w)} = K_\alpha^{(2n)}(0, 0),$$

so $Z_n(0) = C_n$.

Proof sketch. For (ii), condition on the first step from height a to $a \pm 1$: the first step contributes the factor $e^{i\alpha a}$, and the remaining r steps are counted by $K_\alpha^{(r)}(a \pm 1, b)$. The boundary convention encodes the nonnegativity constraint via $K_\alpha^{(r)}(-1, b) = 0$.

For (iii), split a length-$(r+s)$ path at time r. The area functional $\sum_{t=0}^{r+s-1} h_t$ is additive under this concatenation, so the weight factors as the product of the two segment weights. Summing over the intermediate height $b = h_r$ yields the stated composition law. $\square$

Remark 4.3 (Transfer-operator form). *Define an infinite matrix $\mathcal{T}_\alpha$ on $\mathbb{Z}_{\geq 0}$ by*

$$(\mathcal{T}_\alpha)_{a,c} := e^{i\alpha a}\left(\mathbf{1}_{\{c=a+1\}} + \mathbf{1}_{\{c=a-1\}}\right),$$

with the convention $\mathbf{1}_{\{c=-1\}} = 0$. Then the kernel in Definition 4.2 is the rth matrix power:

$$K_\alpha^{(r)}(a, b) = (\mathcal{T}_\alpha^r)_{a,b}.$$

In particular, Lemma 4.1 is the statement that $\mathcal{T}_\alpha^{r+s} = \mathcal{T}_\alpha^r \mathcal{T}_\alpha^s$ and $K_\alpha^{(r+1)} = \mathcal{T}_\alpha K_\alpha^{(r)}$.

Lemma 4.2 (First-return recursion for the area phase). *Let $Z_n(\alpha) := \sum_{w \in \mathcal{D}_n} e^{i\alpha A(w)}$ as in Lemma 4.1. Then $Z_0(\alpha) = 1$, and for $n \geq 1$,*

$$Z_n(\alpha) = \sum_{k=0}^{n-1} e^{i\alpha(2k+1)} Z_k(\alpha) Z_{n-1-k}(\alpha).$$

Equivalently, writing $q := e^{2i\alpha}$ and $C_n(q) := \sum_{w \in \mathcal{D}_n} q^{\mathrm{area}(w)}$, one has $C_0(q) = 1$ and for $n \geq 1$,

$$C_n(q) = \sum_{k=0}^{n-1} q^k C_k(q) C_{n-1-k}(q),$$

the Carlitz–Riordan recursion for the area-refined Catalan numbers.

Proof sketch. Every nonempty Dyck word $w \in \mathcal{D}_n$ admits a unique first-return decomposition

$$w = (\,u\,)\,v,$$

where $u \in \mathcal{D}_k$ and $v \in \mathcal{D}_{n-1-k}$ for a unique $k \in \{0, \ldots, n-1\}$. A direct height bookkeeping shows $A(w) = A(u) + A(v) + (2k+1)$, so $e^{i\alpha A(w)} = e^{i\alpha(2k+1)} e^{i\alpha A(u)} e^{i\alpha A(v)}$. Summing over u and v at fixed k yields the stated recursion for Z_n. The q-form follows from $\mathrm{area}(w) = (A(w) - n)/2$ and the same decomposition; see [16]. $\square$

Corollary 4.1 (Functional equation for the area-refined generating function). *Let $C(q; z) := \sum_{n \geq 0} C_n(q) z^n$, where $C_n(q)$ is as in Lemma 4.2. Then*

$$C(q; z) = 1 + z\, C(q; z)\, C(q; qz).$$

Proof. Multiply the recurrence for $C_n(q)$ in Lemma 4.2 by z^n and sum over $n \geq 1$. Writing $n - 1 = k + m$ gives

$$C(q; z) - 1 = \sum_{k,m \geq 0} q^k C_k(q) C_m(q) z^{k+m+1} = z\, C(q; qz)\, C(q; z).$$

$\square$

Corollary 4.2 (Stieltjes continued fraction). *As a formal power series in z, the solution $C(q; z)$ of Corollary 4.1 admits the continued-fraction expansion*

$$C(q; z) = \cfrac{1}{1 - \cfrac{z}{1 - \cfrac{qz}{1 - \cfrac{q^2 z}{1 - \ddots}}}}.$$

Proof sketch. Rearranging Corollary 4.1 gives $C(q; z) = 1/(1 - z\,C(q; qz))$. Applying the same identity with z replaced by qz yields $C(q; qz) = 1/(1 - qz\,C(q; q^2 z))$, and iterating produces the stated continued fraction. $\square$

Remark 4.4. *Equivalently, define $Z(\alpha; z) := \sum_{n \geq 0} Z_n(\alpha) z^n$. Since $Z_n(\alpha) = e^{i\alpha n} C_n(e^{2i\alpha})$, one has*

$$Z(\alpha; z) = C(e^{2i\alpha}; e^{i\alpha} z),$$

and therefore $Z(\alpha; z)$ satisfies

$$Z(\alpha; z) = 1 + e^{i\alpha} z\, Z(\alpha; z)\, Z(\alpha; e^{2i\alpha} z).$$

Remark 4.5 (Discrete Feynman–Kac viewpoint). *The recursion in Lemma 4.1 is a transfer-matrix formulation for a nearest-neighbour walk with a multiplicative potential term $e^{i\alpha h}$. Under diffusive scaling, this is the discrete analogue of inserting an exponential of a time-integrated potential, as discussed in Section 4.5 [11].*

More generally, one may use any *additive* functional on Dyck histories as a phase source, provided it is computable online from prefix-local growth information. The following proposition records the general form of such functionals.

Proposition 4.1 (Additive phase functionals computable along Dyck growth). *Let w be a Dyck history of semilength n, and let $(X_t)_{t=0}^{2n-1}$ denote the sequence of* prefix-local *growth states along w (e.g. current height and step type). For Dyck histories u, v define concatenation uv as the concatenation of Dyck words.*

A real-valued functional $\Phi(w)$ is additive under Dyck concatenation, i.e. $\Phi(uv) = \Phi(u) + \Phi(v)$, and computable online by a (possibly countable-state) Markov transducer driven by (X_t) with fixed initial internal state $Y_0 = y_*$ for every history, if and only if there exist an internal state process (Y_t) with update rule $Y_{t+1} = F(Y_t, X_t)$ and a real-valued increment function g such that

$$\Phi(w) = \sum_{t=0}^{2n-1} g(Y_t, X_t).$$

Equivalently, defining the augmented prefix-local state $Z_t := (X_t, Y_t)$, one has

$$\Phi(w) = \sum_{t=0}^{2n-1} \varphi(Z_t)$$

for some function φ on the augmented state space.

Proof sketch. Immediate: an online additive transducer emits a per-step output $g(Y_t, X_t)$, whose sum over the growth process defines Φ; conversely, any such per-step sum is computable by an online transducer with internal state (Y_t). $\qquad\square$

Remark 4.6. *In the special case where the transducer carries no internal state (i.e. Y_t is trivial) and the prefix-local state is taken to be the current height h_t, the admissible phase functionals are precisely those of the form*

$$\Phi_f(w) = \sum_t f(h_t),$$

for some function $f : \mathbb{Z}_{\geq 0} \to \mathbb{R}$. Allowing dependence on step type yields the slightly more general form $f(h_t, \Delta h_t)$. The area functional corresponds to the choice $f(h) = h$.

Specializing to the area functional $A(w)$, one may define a complex phase

$$\theta(w) := \alpha\, A(w), \qquad \psi(w) := e^{i\theta(w)},$$

where α is a global scale parameter. No per-path phase assignment is introduced; distinct phases arise solely from differences in the distribution of height over the history.

Given an observable f, the complex amplitude associated with an outcome $x \in \mathcal{X}$ is the coherent sum

$$\Psi(x) := \sum_{w:\, f(w)=x} \psi(w),$$

and observed probabilities are obtained by normalization of squared magnitudes,

$$P(x) = \frac{|\Psi(x)|^2}{\sum_{x' \in \mathcal{X}} |\Psi(x')|^2}.$$

Thus histories that are indistinguishable under the observable f are combined prior to squaring, while distinguishable histories are not. Interference is therefore a generic consequence of assigning complex weights to histories and summing coherently over coarse-grained equivalence classes before applying the Born rule.

Optional: coarse-graining entropy. Appendix D records an optional entropy bookkeeping for coarse-grainings and collapse counts.

4.3   Path integrals and conditioned walks

Dyck paths are random walks conditioned to remain nonnegative and return to zero. Classical results show that, when rescaled appropriately, ensembles of such paths converge to Brownian excursions [12, 10]. Assigning equal weight to all admissible paths yields a discrete analogue of a path integral [9]. More general amplitude assignments may depend on other prefix-local features (e.g. height, step type, or other additive functionals), provided the Dyck constraint is preserved.
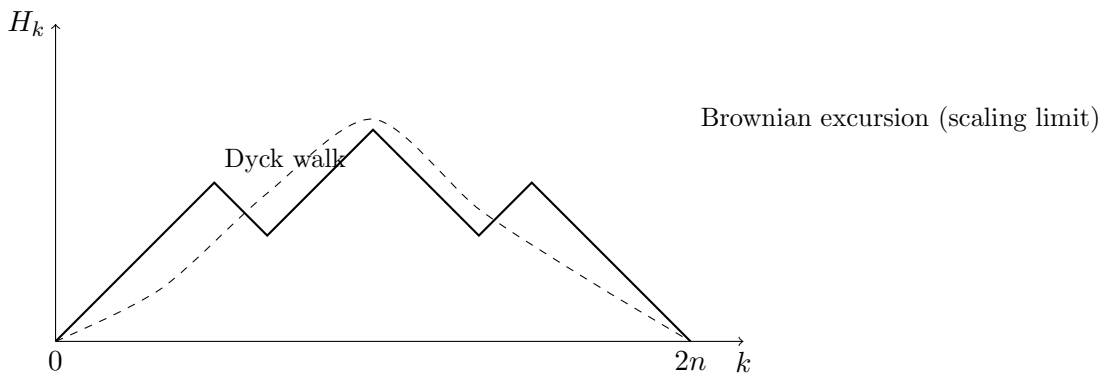

Figure 5: A Dyck path as a nearest-neighbour walk (H_k) constrained to stay nonnegative and return to zero at time $2n$. Under diffusive rescaling of k and H_k, ensembles of such paths converge to Brownian excursions, providing the bridge to the heat and Schrödinger equations discussed in the text.

4.4 Discrete path-integral formulation

The preceding constructions admit a direct interpretation as a discrete path integral on the Catalan light cone. Fix a tier n and an observable $f : \mathcal{D}_n \to \mathcal{X}$, where $\mathcal{X}$ is a finite set of outcomes corresponding to a chosen coarse-graining of histories. Each Dyck path $w \in \mathcal{D}_n$ represents a complete admissible history, and the projection f determines which distinctions between histories are retained and which are discarded.

Define a complex weight for each history by

$$\psi(w) = e^{i\alpha A(w)},$$

where

$$A(w) = \sum_{k=0}^{2n-1} H_w(k)$$

is the discrete height integral introduced above. The amplitude associated with an observable outcome $x \in \mathcal{X}$ is then

$$\Psi(x) = \sum_{w:\, f(w)=x} e^{i\alpha A(w)}.$$

This expression is formally analogous to a path integral [9]: the amplitude is a sum over all admissible histories compatible with the observable outcome, with each history contributing a phase determined by an additive functional. No continuum limit, action functional, or variational principle is assumed at this stage; the structure arises purely from discrete combinatorics.

Several features commonly associated with continuum path integrals are already present:

(i) **Sum over histories.** All admissible Dyck paths consistent with the observable contribute. The Dyck constraint enforces causal admissibility in the same way that restrictions on allowed paths do in relativistic path integrals.

(ii) **Additive phase functional.**

The quantity $A(w)$ is additive under concatenation of path segments and depends only on the local height increments. It therefore plays the role of a discrete action accumulated along the history.

(iii) **Interference from coarse-graining.** Interference arises precisely because the observable f fails to distinguish between certain histories. Histories that are identified by the projection are summed coherently, while those distinguished by the observable are not.

From this perspective, the Catalan lattice provides a discrete realization of the sum-over-histories principle in which both the space of histories and the phase functional are combinatorially well defined. In the next subsection we show that, under appropriate scaling limits, this discrete formulation admits a diffusion (heat) continuum limit (Section 4.6); the same Laplacian generator also yields the free Schrödinger equation under analytic continuation (Section 4.7).

Measurement-like coarse observations may be modeled by choosing observables that retain geometric features of a history (such as transverse displacement at a fixed tier). No such spatial interpretation, however, is required for the formal development.

For readers seeking a concrete intuition for how this discrete sum-over-histories mechanism produces interference, Appendix E sketches a finite thought experiment analogous to the double-slit experiment. The worked example also makes explicit that coherent phase-weighted summation can shift $|\Psi(x)|^2$ substantially away from the raw multiplicities $N(x)$, even at finite tier.

4.5 Scaling of the area phase in the continuum limit

The interference mechanism above assigns each history $w \in \mathcal{D}_n$ a complex weight $\psi(w) = e^{i\alpha A(w)}$ with discrete area functional

$$A(w) := \sum_{k=0}^{2n-1} H_w(k),$$

where $H_w(k)$ is the height after k steps.

To relate this discrete phase to the diffusion scaling limit, introduce the rescaled height process on $[0,1]$,

$$X^{(n)}(\tau) := n^{-1/2} H_w(\lfloor 2n\tau \rfloor), \qquad 0 \le \tau \le 1.$$

Under the standard Dyck-to-Brownian-excursion scaling, $X^{(n)} \Rightarrow X$ in distribution, where X is a Brownian excursion on $[0,1]$.

The discrete area rescales as a Riemann sum:

$$\frac{1}{2n^{3/2}} A(w) = \frac{1}{2n} \sum_{k=0}^{2n-1} n^{-1/2} H_w(k) \implies \int_0^1 X(\tau) \, d\tau.$$

Consequently, a nontrivial continuum phase is obtained by scaling α with n as

$$\alpha_n := \frac{\lambda}{2n^{3/2}},$$

so that

$$e^{i\alpha_n A(w)} \implies \exp\left(i\lambda \int_0^1 X(\tau) \, d\tau \right).$$

This makes explicit that the discrete coherent sum with additive functional $A(w)$ converges to a continuum functional weight. In particular, when one passes from uniform counting of conditioned walks to diffusion limits, inserting the exponential of a time-integrated functional corresponds (at the PDE level) to adding a potential term (via the standard Feynman–Kac mechanism [11]). Setting $\lambda = 0$ recovers the unweighted scaling limit discussed in the next subsection.

4.6 Diffusion limit

Let $n \to \infty$ and rescale time and height by

$$t \mapsto n\tau, \qquad h \mapsto \sqrt{n}\, x.$$

Under this scaling, the rescaled Dyck height process converges in law to a Brownian excursion on $x \ge 0$. At the PDE level, the diffusion part is governed by the heat operator on the half-line, while the Dyck constraint is imposed by conditioning (a Doob transform / Bessel-bridge representation) rather than by a time-homogeneous boundary condition alone. In particular, the corresponding diffusion term on $x > 0$ is the half-line Laplacian,

$$L := \frac{1}{2} \partial_x^2.$$

Remark 4.7 (Discrete generator). *At the lattice level, the (unconditioned) nearest-neighbour walk has the finite-difference generator*

$$(L_{\mathrm{disc}} f)(h) := \tfrac{1}{2}\big(f(h+1) + f(h-1) - 2f(h)\big),$$

with a boundary modification at $h = 0$ if one works on $\mathbb{Z}_{\geq 0}$. Under the diffusive scaling $h = \sqrt{n}\,x$, finite differences converge to second derivatives, so $L = \frac{1}{2}\partial_x^2$ is the continuum limit of this discrete generator.

Moreover, on ℓ^2 (with a corresponding choice of boundary at $h = 0$ when working on $\mathbb{Z}_{\geq 0}$), $-L_{\mathrm{disc}}$ is self-adjoint and thus generates a unitary group $e^{itL_{\mathrm{disc}}}$ solving the discrete free Schrödinger equation $i\partial_t \psi = -L_{\mathrm{disc}}\psi$.

See [12, 10] for standard derivations and precise statements. Appendix C, Section C.3 records a complementary view of the same limit through the covariance structure of the height observable and its Karhunen–Loève modes.

4.7 Schrödinger equation

More formally, let L denote the diffusion generator on $x \geq 0$ with a chosen boundary condition at $x = 0$ (e.g. reflecting/Neumann or absorbing/Dirichlet),

$$L := \frac{1}{2}\,\partial_x^2.$$

The heat semigroup $e^{\tau L}$ governs the base diffusion term; excursion conditioning corresponds to a time-inhomogeneous Doob transform (Remark C.5). Because $-L$ is (under these standard boundary conditions) a self-adjoint nonnegative operator, it generates a unitary group $U_t := e^{-it(-L)} = e^{itL}$. Writing $\psi(t) = U_t \psi(0)$ yields the free Schrödinger equation

$$i\partial_t \psi = -\frac{1}{2}\,\partial_x^2 \psi. \tag{1}$$

Mode-wise phase. Appendix C, Section C.3 shows that, after projecting Dyck histories to the height observable, the resulting signals admit a canonical eigenmode decomposition (Karhunen–Loève modes) of their correlation structure. In the continuum limit, the heat semigroup generated by L is diagonalized by the spectral decomposition of the half-line Laplacian (sine/cosine modes depending on boundary conditions), so each mode evolves by a real decay factor $e^{-k^2\tau/2}$. Under $\tau \mapsto it$ these become pure phases $e^{-ik^2t/2}$. In this sense, analytic continuation replaces diffusive decay by unit-modulus phase rotation of modal coefficients, making coherent cancellation and reinforcement stable under time evolution.

Boundary conditions at $x = 0$ are carried over from the diffusive regime (e.g. reflecting or absorbing), and the choice of boundary does not affect the existence of the continuum limit itself. Thus, a free Schrödinger-type unitary evolution arises here from the same Laplacian generator by passing from a dissipative semigroup to a unitary group; mode-wise, this is the replacement $\tau \mapsto it$ in the spectral representation. This is in line with the classical connection between diffusion and Schrödinger evolution [9, 11]. No separate quantization postulate is required to obtain this unitary evolution from the diffusion generator; interpreting this unitary group as physical quantum dynamics is an additional modeling choice.

5 Locality and Disjoint Commutation

5.1 Disjoint subtrees

Two subtrees of a Dyck tree that share no common ancestor beyond a given prefix are causally independent. Operations localized to one subtree do not affect the other. In the computational

interpretation, this corresponds to independent reductions. In the amplitude interpretation, it corresponds to commuting operators acting on spacelike-separated regions (an analogue of micro-causality). Multiple fine-grained histories may represent the same abstract computation or the same coarse-grained outcome, differing only in the interleaving of independent local updates. When such differences are unobservable (or regarded as irrelevant bookkeeping), one may quotient the history space by the induced equivalence relation, replacing many interleavings by a single equivalence class. This redundancy is structurally analogous to gauge: distinct internal descriptions correspond to the same coarse description.

Operationally, fix an initial tree and consider histories that apply the same multiset of local reductions but differ only in the temporal ordering of reductions supported on disjoint subtrees. By Lemma F.2, these interleavings are related by commuting diamonds. One may therefore treat each equivalence class as a single abstract history (a partial order of events) while reserving genuinely different choices of which reductions occur for the nontrivial branching structure of the multiway reduction graph.

Definition 5.1 (Gauge equivalence generated by commuting diamonds). *Fix an initial tree T_0 and a local rewrite system. Consider the directed multiway reduction graph whose vertices are trees reachable from T_0 and whose edges are single-step reductions. For $m \geq 0$, let $\mathcal{H}_m(T_0)$ be the set of length-m directed paths (reduction histories) starting at T_0.*

An elementary gauge move *replaces a length-2 subpath that traverses one side of a commuting diamond by the other side, i.e. it replaces $T \to T_a \to T_{ab}$ by $T \to T_b \to T_{ba}$ (or vice versa) whenever these four vertices form a diamond as in Figure 6. Let $\sim_g$ denote the equivalence relation on $\mathcal{H}_m(T_0)$ generated by elementary gauge moves.*

Remark (Diamonds vs. linear intervals). In poset language, a commuting diamond is a local obstruction to an interval being chain-like: when two local moves can be performed in either order, the Hasse diagram contains a square and the corresponding interval admits multiple maximal chains. Conversely, "diamond-free" regions correspond to intervals with a unique maximal chain, called *linear intervals* in the Tamari/Dyck/alt-Tamari literature. Thus the gauge quotient advocated here may be viewed as collapsing the redundant permutational degrees of freedom generated by diamonds, while the remaining (non-gauge) branching structure records genuinely different causal dependency patterns. The prevalence of linear intervals—and their invariance across the Tamari, Dyck, and alt-Tamari posets at fixed tier—is analyzed in detail by Chenevière [20].

(See Appendix F, and in particular Lemma F.2, for a formal statement and proof sketch of the corresponding disjoint-commutation property.)

5.2 Collapse and selection

Both computation and amplitude propagation require selection:

- computational reduction chooses a redex,

- measurement-like selection chooses an observable outcome, corresponding to an equivalence class under the chosen projection.

In the Catalan substrate, selection operates locally, refining rather than destroying structure. The global constraint ensures consistency after selection. The formal development of collapse probabilities lies beyond the scope of this paper and is treated here only structurally.
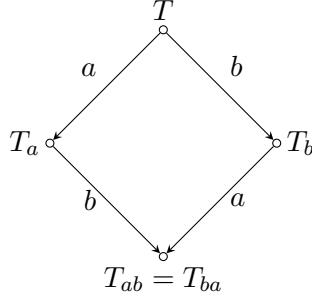
Figure 6: Local diamond for commuting disjoint updates. Starting from a common state T, two spacelike-separated reductions a and b can be applied in either order, yielding intermediate states T_a and T_b but the same final state $T_{ab} = T_{ba}$. The two intermediate events are spacelike-separated: they share a common past (T) and a common future (T_{ab}) but no causal edge between them. This expresses a microcausality analogue on the Catalan substrate: local updates supported on disjoint subtrees commute and differ only by temporal ordering.

5.3 Summary

Locality and disjoint commutation emerge directly from the causal and recursive structure of the Catalan lattice. The same principles underlie both computational reduction and amplitude constructions on the Catalan history space.

6 Discussion and Limitations

The results presented here develop a shared structural framework for causal geometry, a minimal amplitude calculus, and computation. Several limitations should be emphasized:

- Physical constants and interactions are not derived.

- Only free (noninteracting) wave dynamics appears explicitly.

- Collapse probabilities are not fixed uniquely by the structure.

- Lorentz symmetry is discussed only via continuum embeddings; no discrete boost invariance is claimed (Remark C.3).

- The choice of phase/action functional (e.g. Dyck area) is not shown to be unique.

These limitations reflect a deliberate restriction of scope. The goal has been to isolate the minimal recursive structure common to multiple domains, not to provide a complete physical theory.

6.1 Relation to discrete quantum gravity

Similar scaling behavior appears in two-dimensional quantum gravity and random surface models. In particular, Causal Dynamical Triangulations (CDT) enforce a preferred foliation and causal constraint that parallels the prefix order of Dyck paths [2, 3]. In CDT, the continuum limit is taken after summing over causally admissible triangulations. Here the admissible structures are Dyck paths rather than triangulations, but the organizing principle—the restriction to histories that respect a causal growth rule—is closely analogous.

7 Conclusion

This paper treats the Catalan family—Dyck paths, full binary trees, and balanced-parenthesis expressions—as a single discrete history space supporting three complementary readings: causal geometry via the prefix order, computation via application trees and local rewrites, and amplitudes via coherent summation over coarse-grained outcomes. Classical scaling results for conditioned walks provide a continuum comparison in which Dyck ensembles converge to Brownian excursions. The underlying diffusion term is governed by the heat operator on the half-line (with the excursion conditioning represented via a Doob transform), and under analytic continuation one obtains the free Schrödinger equation. The scope is intentionally restricted to this shared structural core: deriving interactions, constants, or a unique collapse/measurement rule requires additional structure beyond what is developed here.

A A Conditional Uniqueness Theorem for the Dyck-Prefix Substrate

This appendix isolates a minimal set of structural axioms under which the Dyck-prefix substrate is not merely an example but is determined uniquely up to isomorphism. The result is interpretation-neutral: it assumes no particular computational semantics (evaluation order, combinators, rewriting), only a ranked causal-growth structure with a one-sided admissibility boundary.

A.1 Ranked growth posets

Definition A.1 (Ranked growth poset). *A ranked growth poset is a triple $(S, \preceq, \mathrm{rk})$ where S is a countable set, $\preceq$ is a partial order on S, and $\mathrm{rk} : S \to \mathbb{N}$ is a rank function such that:*

(i) for every $t \in S$ the set $\{s \in S : s \preceq t\}$ is finite, and

(ii) rk is strictly order-increasing along cover relations.

Write $s \prec t$ when $s \preceq t$ and $s \neq t$, and write $s \lessdot t$ if $s \prec t$ and there is no u with $s \prec u \prec t$ (i.e. t covers s).

Definition A.2 (Two-move height structure). *Let $(S, \preceq, \mathrm{rk})$ be a ranked growth poset with a distinguished root $s_\emptyset \in S$ satisfying $\mathrm{rk}(s_\emptyset) = 0$. A two-move height structure on S consists of a function $h : S \to \mathbb{Z}_{\geq 0}$ (height) with $h(s_\emptyset) = 0$ such that every cover relation $s \lessdot t$ satisfies*

$$\mathrm{rk}(t) = \mathrm{rk}(s) + 1 \qquad and \qquad h(t) = h(s) \pm 1.$$

We call a cover with $h(t) = h(s) + 1$ an up-step and a cover with $h(t) = h(s) - 1$ a down-step.

A.2 Axioms for the Catalan core

The uniqueness theorem below follows from four axioms capturing: (i) discrete single-step growth, (ii) exactly two local move types (up/down), (iii) a one-sided boundary in which down-steps are disabled at height 0, and (iv) an *unfolded* (collision-free) history space.

Definition A.3 (Catalan core axioms). *A ranked growth poset $(S, \preceq, \mathrm{rk})$ with root $s_\emptyset$ and two-move height structure h satisfies the Catalan core axioms if:*

(A1) **(Ranked single-step growth)** *For every cover $s \lessdot t$, one has $\mathrm{rk}(t) = \mathrm{rk}(s) + 1$ and $h(t) = h(s) \pm 1$.*

(A2) **(Local determinism by move type)** *For each $s \in S$, there exists at most one up-step successor $t_\uparrow$ with $s \lessdot t_\uparrow$ and $h(t_\uparrow) = h(s) + 1$, and at most one down-step successor $t_\downarrow$ with $s \lessdot t_\downarrow$ and $h(t_\downarrow) = h(s) - 1$.*

(A3) **(One-sided boundary admissibility)** *For each $s \in S$, an up-step successor exists, while a down-step successor exists iff $h(s) > 0$.*

(A4) **(No collisions / unique history)** *Each $t \in S$ admits a unique saturated chain (cover chain) from the root:*
$$s_\emptyset = s_0 \lessdot s_1 \lessdot \cdots \lessdot s_{\mathrm{rk}(t)} = t.$$

A.3 Dyck-prefix poset

Let $\Sigma = \{+, -\}$. For a word $w = w_1 \cdots w_n \in \Sigma^n$, define the partial-sum height

$$H_w(k) = \sum_{j=1}^{k} \xi(w_j), \qquad \text{where } \xi(+) = +1, \ \xi(-) = -1.$$

Call w *admissible* if $H_w(k) \geq 0$ for all k. Let $\mathcal{C}$ be the set of all admissible words (Dyck prefixes), partially ordered by prefix: $u \preceq v$ iff u is a prefix of v. Let $\ell(w) = n$ be length and $H(w) = H_w(n)$ be final height.

Definition A.4 (Dyck-prefix poset). *The Dyck-prefix poset is $(\mathcal{C}, \preceq, \ell)$ with root ε (the empty word).*

A.4 Uniqueness theorem

Theorem A.1 (Dyck-prefix uniqueness). *Let $(S, \preceq, \mathrm{rk})$ be a ranked growth poset with root $s_\emptyset$ and a two-move height structure h. If S satisfies the Catalan core axioms of Definition A.3, then there exists a unique bijection*
$$\pi : S \to \mathcal{C}$$
such that for every $s \in S$,
$$\ell(\pi(s)) = \mathrm{rk}(s), \qquad H(\pi(s)) = h(s),$$
and π is an order isomorphism:

$$s \preceq t \iff \pi(s) \preceq \pi(t) \quad \text{(prefix order)}.$$

In particular, $(S, \preceq, \mathrm{rk})$ is isomorphic to the Dyck-prefix poset.

Proof. By (A4), each $s \in S$ admits a unique cover chain $s_\emptyset = s_0 \lessdot \cdots \lessdot s_n = s$ where $n = \mathrm{rk}(s)$. Define a word $\pi(s) \in \Sigma^n$ by setting

$$\pi(s)_k = \begin{cases} + & \text{if } h(s_k) = h(s_{k-1}) + 1, \\ - & \text{if } h(s_k) = h(s_{k-1}) - 1. \end{cases}$$

This is well-defined and has length $\ell(\pi(s)) = n$. By construction, the partial sums of $\pi(s)$ coincide with the height along the chain,

$$H_{\pi(s)}(k) = h(s_k) \geq 0 \quad \text{for all } k,$$

23

so $\pi(s)$ is admissible and $\pi(s) \in \mathcal{C}$. Moreover $H(\pi(s)) = H_{\pi(s)}(n) = h(s)$.

We now show that π is bijective. Given any admissible word $w = w_1 \cdots w_n \in \mathcal{C}$, construct a chain in S by starting at $s_0 = s_\emptyset$ and for each $k \geq 1$ taking the successor specified by w_k:

$$
s_k = \begin{cases} \text{the (unique) up-step successor of } s_{k-1} & \text{if } w_k = +, \\ \text{the (unique) down-step successor of } s_{k-1} & \text{if } w_k = -. \end{cases}
$$

Existence and uniqueness follow from (A2)–(A3); admissibility of w ensures that a down-step is only requested when the current height is positive. Let $s := s_n$ be the resulting node at rank n. Then $\pi(s) = w$, proving surjectivity. Injectivity follows from (A4): distinct nodes have distinct cover chains and hence distinct step sequences.

Finally, π preserves order. If $s \preceq t$, then the unique chain to t contains the chain to s as an initial segment, so $\pi(s)$ is a prefix of $\pi(t)$. Conversely, if $\pi(s)$ is a prefix of $\pi(t)$, then the constructed chain for $\pi(t)$ passes through the constructed chain for $\pi(s)$, giving $s \preceq t$. Uniqueness of π is immediate from (A4), since $\pi(s)$ is forced by the unique cover chain to s. □

A.5 Catalan enumeration at completion

To recover the usual Catalan counting, impose a completion boundary condition: completion occurs when the height returns to zero at even rank.

Definition A.5 (Completed histories). *For $n \in \mathbb{N}$, define the set of completed histories at rank $2n$ by*

$$
S_{2n}^{\text{comp}} := \{s \in S : \text{rk}(s) = 2n \text{ and } h(s) = 0\}.
$$

Corollary A.1 (Catalan counting). *Under the hypotheses of Theorem A.1, the number of completed histories satisfies*

$$
\#\left(S_{2n}^{\text{comp}}\right) = C_n = \frac{1}{n+1}\binom{2n}{n},
$$

the nth Catalan number.

Proof. By Theorem A.1, S_{2n}^{comp} is in bijection with admissible words of length $2n$ with final height 0, i.e. Dyck words of semilength n. These are counted by the Catalan number C_n. □

A.6 Quotients and structural sharing

The "no collisions" axiom (A4) asserts that S is an *unfolded* history space: each node encodes a distinct growth history. This does not preclude gauge equivalences or multi-way computation graphs; rather, those arise by quotienting S by an equivalence relation.

Remark A.1 (Quotients and gauge identification). *Let $\sim$ be an equivalence relation on S representing gauge or rewrite identifications. The quotient set $S/\sim$ may exhibit merges (a DAG-like state graph), even if S is collision-free. Theorem A.1 characterizes the unfolded core; quotient structure is encoded by the choice of $\sim$ and acts as an identification of histories rather than a primitive feature of the substrate.*

Remark A.2 (Structural sharing vs. semantic collisions). *Axiom (A4) concerns semantic identity in S (distinct histories are distinct nodes). It is compatible with immutability and structural sharing in implementations (e.g. hash-consing), which may share representation of common substructures without identifying distinct history nodes.*

24

A.7 Scope of the result

Theorem A.1 establishes a core uniqueness statement: given two local move types changing an integer height by ± 1, a one-sided boundary disabling down-steps at height 0, and an unfolded history space, the substrate is forced to be Dyck-prefix order. This statement is independent of additional semantic layers (program interpretations, rewriting dynamics, or amplitude assignments), which can be imposed on top of the substrate without affecting the isomorphism.

B Unfoldings and Covers of Growth Posets

Many natural representations of computation or gauge-identified state spaces exhibit merges: distinct growth histories may lead to the same state, producing a DAG-like multi-way graph rather than a tree. The core uniqueness theorem in Appendix A characterizes the *unfolded* history space. This appendix makes that relationship explicit by defining a canonical unfolding (history cover) for a ranked growth poset and showing that the Catalan uniqueness statement applies upstairs even when merges exist downstairs.

B.1 Growth graphs

Definition B.1 (Rooted ranked growth poset). *A rooted ranked growth poset is a ranked growth poset $(S, \preceq, \mathrm{rk})$ (Definition A.1) equipped with a distinguished root $s_\emptyset \in S$ such that for every $s \in S$ one has $s_\emptyset \preceq s$ (i.e. every node is reachable from the root).*

Definition B.2 (Directed growth graph). *Let $(S, \preceq, \mathrm{rk})$ be a rooted ranked growth poset. Its directed growth graph is the rooted directed graph $G(S) = (V, E, s_\emptyset)$ where $V = S$ and $(s, t) \in E$ iff $s \lessdot t$ (i.e. t covers s). We regard each edge as a single-step growth move.*

Definition B.3 (Move type induced by height). *If $(S, \preceq, \mathrm{rk})$ carries a two-move height structure h (Definition A.2), then each directed edge $s \to t$ in $G(S)$ has a move type*

$$\mathrm{type}(s \to t) \in \{+, -\} \quad \textit{defined by} \quad \mathrm{type}(s \to t) = \begin{cases} + & \textit{if } h(t) = h(s) + 1, \\ - & \textit{if } h(t) = h(s) - 1. \end{cases}$$

B.2 Rooted covers (local isomorphism in one step)

To model "the same local growth rule everywhere" we use a minimal notion of cover: a map that is locally bijective on outgoing edges from each node. This avoids introducing general poset coverings and suffices for the unfolding argument below.

Definition B.4 (Rooted directed cover). *Let $G = (V, E, r)$ and $\widetilde{G} = (\widetilde{V}, \widetilde{E}, \widetilde{r})$ be rooted directed graphs. A function $\varphi : \widetilde{V} \to V$ is a rooted directed cover if:*

(i) $\varphi(\widetilde{r}) = r$;

(ii) for every $\widetilde{v} \in \widetilde{V}$, the map

$$\varphi_* : \mathrm{Out}(\widetilde{v}) \to \mathrm{Out}(\varphi(\widetilde{v})), \qquad (\widetilde{v} \to \widetilde{w}) \mapsto (\varphi(\widetilde{v}) \to \varphi(\widetilde{w}))$$

is a bijection, where $\mathrm{Out}(x) = \{x \to y \in E\}$ denotes the set of outgoing edges from x.

If edges carry move types $\{+, -\}$, we additionally require that φ_* preserves move type (i.e. the bijection matches $+$-edges to $+$-edges and $-$-edges to $-$-edges).

B.3 The canonical unfolding (history cover)

Definition B.5 (Unfolding as rooted path space). *Let $(S, \preceq, \mathrm{rk})$ be a rooted ranked growth poset and let $G(S)$ be its directed growth graph. Define the* unfolding $\widetilde{S}$ *to be the set of all finite directed paths in $G(S)$ starting at the root:*

$$\widetilde{S} := \big\{ (s_0 \to s_1 \to \cdots \to s_n) \; : \; s_0 = s_\emptyset, \; (s_{k-1}, s_k) \in E \big\}.$$

Write $\widetilde{s} = (s_0 \to \cdots \to s_n)$ and define:

  (i) the endpoint *map $\varphi : \widetilde{S} \to S$ by $\varphi(\widetilde{s}) = s_n$;*

  (ii) the rank $\widetilde{\mathrm{rk}}(\widetilde{s}) = n$ *(path length);*

  (iii) the prefix order *on $\widetilde{S}$: $\widetilde{u} \preceq \widetilde{v}$ iff $\widetilde{u}$ is an initial segment (prefix) of $\widetilde{v}$.*

If S has a height function h, define the lifted height $\widetilde{h}(\widetilde{s}) := h(\varphi(\widetilde{s}))$.

Lemma B.1 (The unfolding is collision-free). *Every element $\widetilde{s} \in \widetilde{S}$ has a unique predecessor chain from the root in the prefix order, i.e. $\widetilde{S}$ satisfies the "no collisions / unique history" property (A4) of Definition A.3.*

Proof. By construction, each $\widetilde{s}$ is itself a rooted path $(s_0 \to \cdots \to s_n)$. Its strict prefixes are exactly the initial segments $(s_0 \to \cdots \to s_k)$ for $0 \le k < n$, and these form the unique saturated chain from the root to $\widetilde{s}$ under prefix inclusion. $\square$

Lemma B.2 (The endpoint map is a rooted directed cover). *Let $G(\widetilde{S})$ be the directed growth graph of the unfolding, whose edges append one growth step:*

$$(s_0 \to \cdots \to s_n) \; \to \; (s_0 \to \cdots \to s_n \to s_{n+1}) \quad \text{whenever } s_n \to s_{n+1} \text{ is an edge in } G(S).$$

Then the endpoint map $\varphi : \widetilde{S} \to S$ from Definition B.5 is a rooted directed cover in the sense of Definition B.4. If S carries a two-move height structure, then φ preserves move type.

Proof. Clearly φ maps the length-0 path $(s_\emptyset)$ to $s_\emptyset$. Fix a path $\widetilde{s} = (s_0 \to \cdots \to s_n)$. Outgoing edges from $\widetilde{s}$ in $G(\widetilde{S})$ are in bijection with outgoing edges from s_n in $G(S)$ by appending the corresponding last step $s_n \to s_{n+1}$. Under φ, each appended edge maps to exactly that edge $s_n \to s_{n+1}$, giving a bijection on outgoing edges. If move types are present, appending an up-step or down-step in $\widetilde{S}$ maps to an up-step or down-step in S by Definition B.3, so type is preserved. $\square$

B.4 Dyck-prefix structure upstairs

Proposition B.1 (Lift of the Catalan core axioms). *Suppose $(S, \preceq, \mathrm{rk})$ is a rooted ranked growth poset with a two-move height structure h satisfying axioms (A1)–(A3) of Definition A.3 (ranked single-step growth, local determinism by move type, and one-sided boundary admissibility), but not necessarily (A4). Then the unfolding $(\widetilde{S}, \preceq, \widetilde{\mathrm{rk}})$ with lifted height $\widetilde{h}$ satisfies (A1)–(A4).*

Proof. Axiom (A4) holds by Lemma B.1. For (A1)–(A3), each cover in $\widetilde{S}$ appends exactly one edge of $G(S)$, so ranks increase by one and height changes by ± 1 exactly as in S. Moreover, by local determinism in S, from any endpoint there is at most one $+$-successor and at most one $-$-successor; by Lemma B.2 the same holds in the unfolding at every path. Finally, one-sided boundary admissibility is preserved: a $-$-extension exists in $\widetilde{S}$ precisely when the endpoint height is positive. $\square$

Theorem B.1 (Dyck-prefix characterization of the unfolding)**.** *Under the hypotheses of Proposition B.1, the unfolding $\widetilde{S}$ is (canonically) order-isomorphic to the Dyck-prefix poset (Definition A.4). In particular, completed unfolded histories are counted by Catalan numbers as in Corollary A.1.*

Proof. By Proposition B.1, $\widetilde{S}$ satisfies the full Catalan core axioms (A1)–(A4). The conclusion follows by applying Theorem A.1 to $\widetilde{S}$. $\qquad\square$

Remark B.1 (Canonical quotient and "collisions")**.** *The unfolding comes with a canonical surjection $\varphi : \widetilde{S} \to S$ (the endpoint map). Collisions/merges in S correspond exactly to identifications of distinct unfolded histories:*

$$\widetilde{u} \sim_\varphi \widetilde{v} \quad \Longleftrightarrow \quad \varphi(\widetilde{u}) = \varphi(\widetilde{v}).$$

Thus, as a set of states reachable from the root, S is naturally identified with the quotient $\widetilde{S}/\!\sim_\varphi$. For the distinction between semantic identification and structural sharing in implementations, see Remark A.2.

B.5 A Reduction-Theoretic "Full Uniqueness" Statement

The core uniqueness theorem (Theorem A.1) shows that a collision-free two-move growth system with a one-sided boundary is forced to be Dyck-prefix order. This subsection records a complementary reduction statement: if a canonical notion of *intrinsic state* (defined by future-cone isomorphism) is already a minimal one-counter system, and if the projection to intrinsic state is locally bijective on labeled moves, then the Catalan core is forced as the unfolded normal form.

B.5.1 Future cones and intrinsic-state equivalence

Definition B.6 (Future cone as a rooted directed graph)**.** *Let $(S, \preceq, \mathrm{rk})$ be a rooted ranked growth poset with directed growth graph $G(S) = (S, E, s_\emptyset)$ (Definition B.2). For $s \in S$, define the* future cone *at s to be the rooted directed subgraph*

$$\mathrm{Cone}(s) \ := \ \big(S_s, E_s, s\big),$$

where $S_s = \{t \in S : \ s \preceq t\}$ and $E_s = \{(u,v) \in E : \ u, v \in S_s\}$. If edges in $G(S)$ are labeled by a finite move alphabet (in particular $\{+, -\}$), we regard $\mathrm{Cone}(s)$ as an edge-labeled rooted directed graph.

Definition B.7 (Cone isomorphism and intrinsic-state equivalence)**.** *Assume edges are labeled by move type in $\{+, -\}$. For $s, t \in S$, write $s \equiv t$ if there exists a rooted directed graph isomorphism*

$$\psi : \mathrm{Cone}(s) \ \cong \ \mathrm{Cone}(t)$$

sending root to root and preserving move labels. This defines an equivalence relation $\equiv$ on S, called intrinsic-state equivalence. Let $M := S/\!\equiv$ be the set of equivalence classes, with root $m(s_\emptyset) \in M$, and write

$$m : S \to M, \qquad m(s) = [s]_\equiv$$

for the canonical projection.

Remark B.2 (Relocatable futures)**.** *The equivalence relation $\equiv$ captures a precise form of relocatability: states are indistinguishable if and only if their reachable futures are isomorphic as rooted labeled growth graphs. The quotient $M = S/\!\equiv$ is a canonical "coarsest" state descriptor that preserves the full future growth structure.*

B.5.2 Intrinsic dynamics and the cover hypothesis

Definition B.8 (Intrinsic transition graph). *Let $G(S)$ be labeled by $\{+,-\}$. Define a rooted labeled directed graph $G(M)$ on M by declaring a labeled edge $x \to_{\pm} y$ to exist if there are $s,t \in S$ such that $s \lessdot t$ is a $\pm$-labeled edge of $G(S)$ and $m(s) = x$, $m(t) = y$.*

Definition B.9 (One-counter intrinsic dynamics). *We say $(S, \preceq, \mathrm{rk})$ has one-counter intrinsic dynamics if there exists a bijection*

$$\iota : M \;\to\; \mathbb{Z}_{\geq 0}$$

with $\iota(m(s_\emptyset)) = 0$ such that, for every intrinsic state $x \in M$ with $\iota(x) = k$:

(i) (***Two primitive moves***) *there exists exactly one $+$-successor y_+ of x in $G(M)$ with $\iota(y_+) = k + 1$;*

(ii) (***One-sided boundary***) *there exists a $-$-successor y_- of x in $G(M)$ iff $k > 0$, and in that case $\iota(y_-) = k - 1$;*

(iii) (***No other intrinsic moves***) *x has no other outgoing edges in $G(M)$ besides $x \to_+ y_+$ and (when $k > 0$) $x \to_- y_-$.*

Equivalently, $G(M)$ is isomorphic (as a rooted labeled graph) to the standard one-counter graph on $\mathbb{Z}_{\geq 0}$ with edges $k \to_+ k + 1$ for all k and edges $k \to_- k - 1$ for $k > 0$.

Remark B.3 (Minimality content). *Definition B.9 should be read as a minimality hypothesis: the intrinsic descriptor $M = S/\equiv$ is already a single nonnegative integer, and it admits exactly two primitive move types with a one-sided boundary at 0.*

Definition B.10 (Cover-consistency of the intrinsic projection). *Assume edges are labeled by $\{+,-\}$. We say the intrinsic projection $m : S \to M$ is cover-consistent if it is a rooted directed cover (Definition B.4) from the labeled growth graph $G(S)$ to the intrinsic graph $G(M)$ (Definition B.8), i.e. for every $s \in S$ the induced map on outgoing edges $\mathrm{Out}(s) \to \mathrm{Out}(m(s))$ is a label-preserving bijection.*

Remark B.4. *Under the one-counter identification $\iota : M \to \mathbb{Z}_{\geq 0}$ of Definition B.9, cover-consistency of m is equivalent to requiring that the composite $h := \iota \circ m : S \to \mathbb{Z}_{\geq 0}$ is a rooted directed cover from $G(S)$ to the standard one-counter graph on $\mathbb{Z}_{\geq 0}$.*

B.5.3 Reduction to the Dyck-prefix normal form

Theorem B.2 (Reduction to a Dyck-prefix cover). *Let $(S, \preceq, \mathrm{rk})$ be a rooted ranked growth poset whose directed growth graph $G(S)$ is labeled by move type in $\{+,-\}$. Assume:*

(H1) (***Intrinsic-state quotient***) *intrinsic-state equivalence $\equiv$ is defined by label-preserving cone isomorphism as in Definition B.7, with quotient $m : S \to M$;*

(H2) (***One-counter intrinsic dynamics***) *S satisfies Definition B.9;*

(H3) (***Cover consistency***) *the intrinsic projection m is a rooted directed cover as in Definition B.10;*

(H4) (***Tiered single-step growth***) *for every cover $s \lessdot t$, $\mathrm{rk}(t) = \mathrm{rk}(s) + 1$.*

Let $\widetilde{S}$ be the unfolding (history cover) of S (Definition B.5) with endpoint map $\varphi : \widetilde{S} \to S$. Then $\widetilde{S}$ is (canonically) order-isomorphic to the Dyck-prefix poset (Definition A.4), and hence S is a quotient (folding) of a Dyck-prefix cover via φ (Remark B.1).

Proof. Define a height function on S by composing the intrinsic-state projection with the one-counter identification,

$$h(s) \; := \; \iota(m(s)) \in \mathbb{Z}_{\geq 0}.$$

By cover consistency (Definition B.10) and one-counter intrinsic dynamics (Definition B.9), each $s \in S$ has exactly one outgoing +-edge, and it has an outgoing −-edge iff $h(s) > 0$. Moreover, because m is label-preserving and ι identifies $G(M)$ with the standard one-counter graph, along any cover edge $s \lessdot t$ one has $h(t) = h(s) + 1$ for a +-edge and $h(t) = h(s) - 1$ for a −-edge. Together with the tier assumption $\mathrm{rk}(t) = \mathrm{rk}(s) + 1$, this shows that S admits a two-move height structure satisfying axioms (A1)–(A3) of Definition A.3.

Applying Theorem B.1 now yields that the unfolding $\widetilde{S}$ is Dyck-prefix order-isomorphic. The quotient statement for S is then exactly Remark B.1. $\qquad\square$

Remark B.5 (What is and is not proved). *Theorem B.2 is a "full uniqueness" statement in the reduction sense: once relocatable futures are formalized via cone isomorphism and the intrinsic state space is assumed to be a one-counter with two primitive moves, together with the cover-consistency hypothesis (no hidden multiplicity in the projection m), the Catalan substrate is forced as the unfolded normal form. What is not claimed is that all reasonable substrates satisfy these minimality hypotheses; establishing that requires separate domain-specific arguments.*

B.6 Interpretive takeaway

Theorems A.1 and B.1 together support the following robust core statement: whenever a ranked two-move growth system with a one-sided boundary is present, the unfolded history space is forced to be Dyck-prefix order, and any merged multi-way representation is a quotient of that Catalan cover.

C Coordinate Charts and Continuum Comparisons

This appendix collects optional coordinate embeddings and continuum comparisons used for intuition; the combinatorial results in the main text do not depend on these constructions.

C.1 Coordinate charts on the Catalan cone

Remark C.1 (Notation hygiene). *To avoid collisions, the* tier *(semilength) of a completed history is denoted by n. A prefix length is denoted by $k \in \{0, 1, \ldots, 2n\}$. Within this subsection only, the symbols (t_k, x_k) denote an embedded spacetime chart derived from cumulative counts (Definition C.1), and should not be confused with the tier index n used elsewhere.*

The Catalan cone as the master object. Let $\mathcal{C}$ denote the set of Dyck prefixes (balanced-parentheses *prefixes* that never go below height 0), partially ordered by extension: $p \preceq q$ iff q has prefix p. A completed history is a maximal element $w \in \mathcal{D}_n \subset \mathcal{C}$ of semilength n. For any prefix $p \in \mathcal{C}$, the future

$$\mathcal{C}(p) \; := \; \{\, q \in \mathcal{C} : p \preceq q \,\}$$

is canonically a "local cone" rooted at p: the same growth law, re-centered. Thus there is a single substrate $\mathcal{C}$ (and its re-rootings), and different "cones" arise from different coordinate charts or coarse-grainings of this same object.

Two cumulative counts and a light-cone chart. The most rigid chart on $\mathcal{C}$ is obtained by tracking the cumulative numbers of opens and closes.

Definition C.1 (Null counts and embedded coordinates)**.** *Fix a Dyck word $w \in \mathcal{D}_n$, and let $w[1\!:\!k]$ denote its length-k prefix. Define*

$$u(k) \; := \; \#\{ \, (\; in \; w[1\!:\!k]\}, \qquad v(k) \; := \; \#\{ \,) \; in \; w[1\!:\!k]\}.$$

The Dyck admissibility constraint is $u(k) \geq v(k)$ for all k, and completion is $u(2n) = v(2n) = n$. Define the height (frontier) process

$$H(k) \; := \; u(k) - v(k) \; \geq \; 0,$$

and the embedded "spacetime" coordinates

$$t_k \; := \; \frac{u(k) + v(k)}{2} \; = \; \frac{k}{2}, \qquad x_k \; := \; \frac{u(k) - v(k)}{2} \; = \; \frac{H(k)}{2}.$$

Equivalently $u = t_k + x_k$ and $v = t_k - x_k$ (a discrete null-coordinate form).

Under this embedding, each symbol advances time and changes space by one unit (up to the $1/2$ normalization):

$$(: \; (t,x) \mapsto (t + \tfrac{1}{2}, \; x + \tfrac{1}{2}), \qquad) : \; (t,x) \mapsto (t + \tfrac{1}{2}, \; x - \tfrac{1}{2}).$$

Hence the path stays inside the cone $|x_k| \leq t_k$, with the boundary $x_k = 0$ representing zero frontier (no outstanding opens).

Why "return to 0" is not "return to the origin." The completion constraint $H(2n) = 0$ means only that the *imbalance* vanishes: every open has been matched by a close. In spacetime coordinates, the endpoint is

$$(t_{2n}, x_{2n}) \; = \; (n, 0),$$

not $(0, 0)$. Thus a history expands monotonically in t (prefix length grows), while the spatial coordinate x is a *frontier variable* that eventually returns to 0 because no unfinished structure may remain at completion.

Pairs, trees, and S-expressions are identical structure. A Dyck word w can be read as a parenthesized S-expression skeleton, and it already *is* a rooted ordered tree: matched parenthesis pairs are nodes; containment defines parent/child; and left-to-right order in the string gives sibling order. For example, $w = (()())$ has one outer pair (the root) containing two inner pairs (two leaves). Under this identification, the height $H(k)$ is the number of currently-open pairs—the size of the *active frontier* of the tree under construction.

Evaluation "return" as frontier discharge. If evaluation is recorded at the level of control (continuations), then entering a subproblem pushes a context frame and finishing it pops that frame. In a well-bracketed evaluation regime, this push/pop trace is Dyck, and the same counts $(u(k), v(k))$ track control events. The embedded coordinate x_k therefore measures continuation depth (pending contexts), and the return to $x = 0$ at termination is the emptying of the continuation stack: no pending contexts remain. Value return is mediated by this control return; the Dyck "return" is fundamentally the discharge of outstanding obligations.

Breadth as a different projection (history-level, not frontier-level). Statistics such as breadth $r(w)$ summarize a *completed* history by the maximum size of a constant-depth slice in its associated tree. This is a coarse-graining of w (many distinct histories share the same (n, r)), and it should be distinguished from the frontier coordinate x_k, which is an instantaneous depth/obligation variable along a single prefix trajectory.

Summary of the two readings. There is one substrate $\mathcal{C}$ (and its re-rooted futures $\mathcal{C}(p)$). Two useful "cone" pictures arise from: (i) the embedded prefix trajectory (t_k, x_k) derived from null counts (pathwise frontier dynamics), and (ii) history-level projections such as $(n, r(w))$ (coarse geometric envelope). The pairs/tree/S-expression view does not introduce a new object; it is an identity of representations of the same Catalan structure.

C.2 Dyck Coordinates, Lorentz Geometry, and Computational Proper Time

Remark C.2 (Indices and coordinate conventions). *Throughout, n denotes the tier (semilength) of a completed Dyck history. Within this subsection, $k \in \{0, 1, \ldots, 2n\}$ denotes a step index along a single history, and m denotes the number of collapse events (local redex contractions) performed by a chosen evaluation strategy.*

A Dyck history $w \in \mathcal{D}_n$ induces the height process $H(k)$ of Definition C.1. The corresponding embedded coordinates are $t_k = k/2$ and $x_k = H(k)/2$, so that each parenthesis advances time by $\frac{1}{2}$ and changes the transverse coordinate by $\pm\frac{1}{2}$:

$$\texttt{(} : \ (t, x) \mapsto (t + \tfrac{1}{2}, \ x + \tfrac{1}{2}), \qquad \texttt{)} : \ (t, x) \mapsto (t + \tfrac{1}{2}, \ x - \tfrac{1}{2}).$$

For any walk with steps $(\Delta t, \Delta x) = (\frac{1}{2}, \pm\frac{1}{2})$ one has the kinematic cone bound $|x_k - x_0| \leq t_k - t_0$. In the Dyck case, the additional constraint is one-sided: $x_k \geq 0$ for all k, together with the endpoint condition $x_{2n} = 0$. Thus Dyck histories occupy the right half of a discrete light cone and return to the axis only at completion.

Introduce discrete null coordinates (compare Definition C.1)

$$u := t + x, \qquad v := t - x.$$

In continuum $(1 + 1)$-dimensional Minkowski space, a Lorentz boost with rapidity η acts linearly as

$$u' = e^\eta u, \qquad v' = e^{-\eta} v, \tag{2}$$

and transforming back to (t, x) yields the standard Lorentz transformation

$$t' = \gamma(t - v_L x), \qquad x' = \gamma(x - v_L t), \tag{3}$$

where

$$\gamma = \frac{1}{\sqrt{1 - v_L^2}}, \qquad v_L = \tanh \eta,$$

in units $c = 1$. The Minkowski interval

$$\mathrm{d}s^2 = \mathrm{d}t^2 - \mathrm{d}x^2 \tag{4}$$

is invariant under (3). In this sense the step rule supplies a discrete null-step kinematics, while the Dyck constraint supplies the boundary and return conditions selecting the Catalan ensemble. We emphasize that generic nontrivial boosts do not preserve the discrete Dyck lattice itself (the counts u, v are integers), so the Lorentz discussion here is a continuum comparison for the embedded coordinates rather than a discrete symmetry claim.

Remark C.3 (No nontrivial boost preserves the Dyck lattice)**.** *In the embedded chart, u and v are integer-valued null counts. A Lorentz boost acts by $(u, v) \mapsto (e^\eta u, e^{-\eta} v)$ as in Equation (2). If such a boost maps $\mathbb{Z}^2$ to itself, then e^η and $e^{-\eta}$ must both be integers, hence $e^\eta e^{-\eta} = 1$ forces $e^\eta = 1$ and $\eta = 0$. Thus there is no exact discrete boost invariance of the integer lattice of null counts (beyond the identity; discrete reflections correspond to separate, non-boost symmetries).*

Computational proper time. A reduction history carries an intrinsic progress parameter given by the count of collapse events. Let m be the number of local redex contractions performed by an evaluation strategy up to a given stage, and define the *computational proper time*

$$\tau := \alpha\, m, \tag{5}$$

where $\alpha > 0$ is the characteristic scale associated with a single collapse. In continuum Minkowski space, a parametrized world-line $(t(s), x(s))$ admits a proper-time functional

$$\left(\frac{\mathrm{d}\tau}{\mathrm{d}s}\right)^2 = \left(\frac{\mathrm{d}t}{\mathrm{d}s}\right)^2 - \left(\frac{\mathrm{d}x}{\mathrm{d}s}\right)^2, \tag{6}$$

which is Lorentz-invariant under (3). In the present discrete setting, Equation (5) is simply a well-defined event-count parameter; the analogy is that collapse count plays the role of a proper-time progress variable along a chosen computational history.

C.3 Projection to Height Dynamics and Correlation Structure

Let $\mathcal{C}$ denote the set of Dyck prefixes, i.e. finite words in $\{(,)\}$ whose height never falls below zero. Each prefix $p \in \mathcal{C}$ has an associated height $h(p) \in \mathbb{Z}_{\geq 0}$ given by the net excess of opening over closing parentheses. Completed Dyck words of semilength n form the subset $\mathcal{D}_n \subset \mathcal{C}$ of prefixes of length $2n$ with $h = 0$.

The Catalan growth rule specifies admissible extensions: from a prefix p, one may append "(" unconditionally, or ")" provided $h(p) > 0$. To describe this probabilistically, it is convenient to separate the base process from the Dyck-conditioned ensemble.

Base height process. Let $(H_t)_{t \geq 0}$ be a simple symmetric random walk on $\mathbb{Z}$ with increments ± 1. This walk is time-homogeneous and Markov. Its sample paths may be viewed as unconstrained height sequences, without regard to the Dyck condition.

Dyck conditioning. The Dyck ensemble of length $T = 2n$ is obtained by conditioning the base walk on the event

$$\{H_t \geq 0 \text{ for all } t \leq T,\ H_T = 0\}.$$

Under this conditioning, the law of $(H_t)_{t=0}^T$ is uniform on Dyck paths of semilength n. Equivalently, the conditioned process may be represented via a Doob h-transform (or bridge kernel) of the base walk. In this representation, the height process remains Markov but becomes time-inhomogeneous due to the global conditioning. Each completed Dyck word $p \in \mathcal{D}_n$ corresponds uniquely to a sample path

$$(h_0, h_1, \ldots, h_T), \qquad h_0 = h_T = 0,\ h_t \geq 0,$$

drawn from this conditioned law.

Lemma C.1 (Conditioned transition probabilities)**.** *For integers $r \geq 0$ and $h \geq 0$, let $B(r, h)$ denote the number of nonnegative ± 1 paths of length r that start at height h and end at 0 (so $B(r, h) = 0$ unless $r \geq h$ and $r \equiv h$ (mod 2)). Then the Dyck conditioning above yields a time-inhomogeneous Markov chain. Writing*

$$\mathcal{E} := \{H_s \geq 0 \text{ for all } s \leq T, \ H_T = 0\},$$

its one-step transition probabilities are, for $0 \leq t < T$ and $h \geq 0$ with $B(T - t, h) > 0$,

$$\mathbb{P}(H_{t+1} = h + 1 \mid H_t = h, \ \mathcal{E}) \ = \ \frac{B(T - t - 1, h + 1)}{B(T - t, h)},$$

$$\mathbb{P}(H_{t+1} = h - 1 \mid H_t = h, \ \mathcal{E}) \ = \ \frac{B(T - t - 1, h - 1)}{B(T - t, h)},$$

with the convention $B(\cdot, -1) = 0$ (so the down-step probability is 0 at $h = 0$). Moreover, $B(r, h)$ is given explicitly by the ballot-number formula of Lemma 2.1 (taking r as the remaining step budget).

Remark C.4 (Closed form)**.** *Writing $r := T - t$ and assuming $B(r, h) > 0$, Lemma 2.1 gives the explicit probabilities*

$$\mathbb{P}(H_{t+1} = h + 1 \mid H_t = h, \ \mathcal{E}) = \frac{(h + 2)(r - h)}{2r(h + 1)}, \qquad \mathbb{P}(H_{t+1} = h - 1 \mid H_t = h, \ \mathcal{E}) = \frac{h(r + h + 2)}{2r(h + 1)}.$$

In particular, the conditional drift is

$$\mathbb{E}[H_{t+1} - H_t \mid H_t = h, \ \mathcal{E}] = \frac{r - h(h + 2)}{r(h + 1)}.$$

Remark C.5 (Drift scaling and the Bessel-bridge limit)**.** *Fix semilength n so that $T = 2n$. Consider the rescaled time parameter $\tau := t/n \in [0, 2]$ and the rescaled height $X^{(n)}(\tau) := n^{-1/2} H_{\lfloor n\tau \rfloor}$. If H_t is of order $\sqrt{n}$, write $h = \lfloor \sqrt{n}\, x \rfloor$ and note that $r = T - t \approx n(2 - \tau)$. Substituting into the exact drift formula in Remark C.4 gives the formal approximation*

$$\mathbb{E}\Big[X^{(n)}\big(\tau + \tfrac{1}{n}\big) - X^{(n)}(\tau) \mid X^{(n)}(\tau) \approx x, \ \mathcal{E}\Big] \approx \frac{1}{n}\left(\frac{1}{x} - \frac{x}{2 - \tau}\right),$$

exhibiting a repulsive term $1/x$ from the hard wall at 0 together with an attractive term $-x/(2 - \tau)$ enforcing return to 0 at time horizon 2. This matches the time-inhomogeneous drift of the 3-dimensional Bessel bridge representation of Brownian excursion [14, 17].

More explicitly, a 3-dimensional Bessel bridge $(X_\tau)_{0 \leq \tau < 2}$ from 0 to 0 over time horizon 2 solves the SDE

$$\mathrm{d}X_\tau = \mathrm{d}B_\tau \ + \ \left(\frac{1}{X_\tau} - \frac{X_\tau}{2 - \tau}\right) \mathrm{d}\tau,$$

where the singular drift $1/X_\tau$ encodes conditioning to stay nonnegative and the term $-X_\tau/(2 - \tau)$ encodes the bridge-to-0 constraint.

Remark C.6 (Doob transform and completion weighting)**.** *Let P be the kernel of the simple symmetric walk killed upon attempting to step from 0 to -1. Equivalently, adjoin a cemetery state $\dagger$ and take $P(0, 1) = P(0, \dagger) = 1/2$ and $P(h, h \pm 1) = 1/2$ for $h > 0$, then restrict to $\mathbb{Z}_{\geq 0}$ (so P is sub-Markov at 0). Writing again $r := T - t$, the function $h_r(h) := B(r, h)$ is the number of admissible completions from height h in r remaining steps and satisfies the backward recursion*

of Lemma C.2. The conditioned chain in Lemma C.1 is exactly the time-inhomogeneous Doob h-transform of P with h_r:

$$\mathbb{P}(H_{t+1} = h \pm 1 \mid H_t = h, \ \mathcal{E}) = P(h, h \pm 1) \frac{h_{r-1}(h \pm 1)}{h_r(h)} = \frac{B(r-1, h \pm 1)}{B(r, h)},$$

so the next step is chosen with probability proportional to the number of admissible futures after taking that step.

Proof sketch. Because the base walk is simple symmetric, all length-T paths have equal probability 2^{-T}, so conditioning yields the uniform distribution on admissible paths. Given $H_t = h$, the conditional probability of an up step is proportional to the number of admissible completions from height $h + 1$ in the remaining $T - t - 1$ steps, and similarly for a down step; normalizing gives the stated ratios. The explicit binomial difference for $B(r, h)$ follows from the reflection principle / ballot theorem [16]. □

Lemma C.2 (Recurrence for completion counts). *The completion counts $B(r, h)$ satisfy*

$$B(0, 0) = 1, \qquad B(0, h) = 0 \text{ for } h > 0,$$

and for $r \geq 1$ and $h \geq 0$,

$$B(r, h) = B(r - 1, h - 1) + B(r - 1, h + 1),$$

with the convention $B(r, -1) := 0$.

Proof. Decompose a nonnegative length-r path from height h to 0 by its first step. After a down step (to $h - 1$) or up step (to $h + 1$), there remain $r - 1$ steps to reach 0 without crossing below 0. Summing these disjoint cases gives the recurrence; the boundary convention $B(r, -1) = 0$ enforces the nonnegativity constraint. □

Lemma C.3 (Catalan-triangle height marginal). *Let $T = 2n$ and consider the uniform measure on Dyck paths of semilength n. For $0 \leq t \leq T$ and $h \geq 0$, the number of Dyck paths with $H_t = h$ factors as*

$$\#\{w \in \mathcal{D}_n : H_w(t) = h\} = B(t, h) \, B(T - t, h),$$

and hence

$$\mathbb{P}(H_t = h) = \frac{B(t, h) \, B(T - t, h)}{C_n}, \qquad C_n = B(T, 0).$$

Proof sketch. Split a Dyck path at time t. The prefix from 0 to h of length t and the suffix from h to 0 of length $T - t$ must both stay nonnegative. By time reversal, the number of admissible prefixes from 0 to h of length t equals $B(t, h)$, and admissible suffixes are counted by $B(T - t, h)$. Concatenating a prefix and suffix yields a Dyck path with $H_t = h$, and this factorization is bijective. □

Definition C.2 (Nonnegative bridge counts). *For $r \geq 0$ and $a, b \in \mathbb{Z}_{\geq 0}$, write $B(r; a \to b)$ for the number of length-r ± 1 paths that start at height a, end at height b, and remain nonnegative throughout. In particular, the completion counts in Lemma C.1 are $B(r, h) = B(r; h \to 0)$.*

Lemma C.4 (Ballot-number bridge count). *For $r \geq 0$ and $a, b \in \mathbb{Z}_{\geq 0}$,*

$$B(r; a \to b) = \binom{r}{\frac{r + b - a}{2}} - \binom{r}{\frac{r + b + a}{2} + 1},$$

with the convention $\binom{r}{k} = 0$ when $k \notin \{0, 1, \dots, r\}$ or k is not an integer. In particular, $B(r, h) = B(r; h \to 0)$ agrees with the completion count of Lemma 2.1.

34

Proof sketch. Count all length-r ± 1 paths from a to b and subtract those that ever hit -1. Reflect the initial segment up to the first visit to -1; this gives a bijection between paths from a to b that hit -1 and unconstrained paths from $-a - 2$ to b. Evaluating both counts yields the stated binomial difference; see [16]. □

Lemma C.5 (Two-time height marginal). *Let $T = 2n$ and consider the uniform measure on Dyck paths of semilength n. For $0 \leq s \leq t \leq T$ and $a, b \geq 0$, the number of Dyck paths with $H_s = a$ and $H_t = b$ factors as*

$$\#\{w \in \mathcal{D}_n : H_w(s) = a, \ H_w(t) = b\} = B(s; 0 \to a) \, B(t - s; a \to b) \, B(T - t; b \to 0),$$

and hence

$$\mathbb{P}(H_s = a, \ H_t = b) = \frac{B(s; 0 \to a) \, B(t - s; a \to b) \, B(T - t; b \to 0)}{C_n}, \qquad C_n = B(T; 0 \to 0).$$

Proof sketch. Split a Dyck path into three segments: from time 0 to s (height $0 \to a$), from s to t (height $a \to b$), and from t to T (height $b \to 0$). The Dyck constraint implies that each segment stays nonnegative, so concatenation gives a bijection between Dyck paths realizing $(H_s, H_t) = (a, b)$ and triples of nonnegative segments counted by the product above. □

Lemma C.6 (Multi-time factorization and Markov kernel). *Let $T = 2n$ and consider the uniform measure on Dyck paths of semilength n. Fix times $0 = t_0 \leq t_1 \leq \cdots \leq t_m \leq T$ and heights $h_0 := 0, h_1, \ldots, h_m \in \mathbb{Z}_{\geq 0}$. Then*

$$\#\{w \in \mathcal{D}_n : H_w(t_j) = h_j \text{ for all } j = 1, \ldots, m\} = \Big(\prod_{j=1}^m B(t_j - t_{j-1}; h_{j-1} \to h_j) \Big) B(T - t_m; h_m \to 0).$$

In particular, $(H_t)_{0 \leq t \leq T}$ under the uniform Dyck measure is a time-inhomogeneous Markov chain on $\mathbb{Z}_{\geq 0}$ with transition probabilities, for $0 \leq s \leq t \leq T$,

$$\mathbb{P}(H_t = b \mid H_s = a) = \frac{B(t - s; a \to b) \, B(T - t; b \to 0)}{B(T - s; a \to 0)},$$

whenever $B(T - s; a \to 0) > 0$.

Proof sketch. Split a Dyck path into consecutive nonnegative bridge segments between the prescribed times; concatenation is bijective and multiplies counts. The Markov kernel follows by dividing the two-time count by the one-time marginal (Lemma C.3). □

Correlation structure. Consider the ensemble of height paths of fixed length T, distributed according to the Dyck-conditioned law. Define the mean and covariance functions

$$\mu_t := \mathbb{E}[H_t], \qquad C(s, t) := \mathbb{E}[(H_s - \mu_s)(H_t - \mu_t)], \qquad 0 \leq s, t \leq T.$$

Remark C.7 (Explicit mean and covariance formulas). *By Lemma C.3,*

$$\mu_t = \sum_{h \geq 0} h \, \frac{B(t, h) \, B(T - t, h)}{C_n}.$$

35

By Lemma C.5,

$$\mathbb{E}[H_s H_t] = \sum_{a,b \geq 0} ab \, \frac{B(s; 0 \to a) \, B(t-s; a \to b) \, B(T-t; b \to 0)}{C_n},$$

and hence $C(s,t) = \mathbb{E}[H_s H_t] - \mu_s \mu_t$. All bridge counts $B(\cdot; \cdot \to \cdot)$ admit explicit binomial expressions by Lemma C.4.

The covariance kernel C is a symmetric positive operator on the finite-dimensional space $\mathbb{R}^{T+1}$ and captures the second-order temporal structure induced by the Dyck constraint. It admits an eigen-decomposition

$$\sum_{t=0}^{T} C(s,t) \, v_t^{(k)} = \lambda_k \, v_s^{(k)},$$

yielding an orthogonal family of temporal modes. Any centered height profile admits the expansion

$$H_t - \mu_t = \sum_k \xi_k \, v_t^{(k)}, \qquad \mathbb{E}[\xi_k \xi_\ell] = \lambda_k \, \delta_{k\ell}.$$

In this precise sense, the eigenvalues λ_k constitute the spectrum of temporal correlations induced by the Dyck-conditioned dynamics, and the associated eigenvectors provide a canonical modal decomposition (Karhunen–Loève expansion) of Dyck height signals.

Scaling limit. Under diffusive scaling, the base random walk converges to Brownian motion on $\mathbb{R}$. The Dyck-conditioned law converges to Brownian excursion, which may be described equivalently as Brownian motion conditioned to remain nonnegative and return to zero, or via a Doob transform / Bessel-bridge representation [17, 14] (compare Remark C.5). The resulting continuum evolution is governed by a second-order differential operator on $\mathbb{R}_{\geq 0}$ whose drift and boundary behavior encode the conditioning. In related unconditioned or bridge settings, the associated covariance eigenfunctions are explicitly sinusoidal; for the excursion case, the exact eigenstructure is more subtle, though the dominant modes often resemble sine-like functions away from boundaries.

Thus, the appearance of modal structure follows directly from the projection of Catalan growth dynamics to the height observable and the standard spectral analysis of the resulting correlation kernel, without the introduction of additional postulates beyond the Dyck-conditioned height process and standard spectral analysis.

Remark C.8 (Self-similarity and reference frames). *The Dyck prefix structure is recursively self-similar: every prefix is itself the root of a complete Catalan subtree. Consequently, distinctions such as parent and child, past and future, or global and local history are not intrinsic to the substrate but arise only after fixing a reference root, which induces a causal orientation. The projected height dynamics, their conditioning, and their scaling limits are invariant under such re-rootings.*

D   Additional Technical Notes

D.1   Entropy of coarse-graining and information rate

Fix a tier n and an observable (deterministic coarse-graining) $f : \mathcal{D}_n \to \mathcal{X}$. For $x \in \mathcal{X}$ write

$$N(x) := \#\{w \in \mathcal{D}_n : f(w) = x\},$$

so that $f^{-1}(x)$ is the equivalence class of histories identified as the same outcome.

Multiplicity entropy. Define the (microcanonical) entropy of the full ensemble at tier n by

$$S_n := \log \#(\mathcal{D}_n),$$

and the conditional entropy of an outcome x by

$$S(x) := \log N(x).$$

The information eliminated by selecting outcome x is the entropy drop

$$\Delta S(x) := S_n - S(x) = \log\Big(\frac{\#(\mathcal{D}_n)}{N(x)}\Big).$$

(Any logarithm base may be used; base 2 yields units of bits.)

Remark D.1 (Retrospective vs. prospective counts). *The multiplicity entropy $S(x) = \log N(x)$ measures how many fine-grained histories are identified as the same outcome at tier n. A complementary forward-looking quantity is the number of admissible continuations of a realized prefix into higher tiers (the size of its local cone; see Section 2.9), which may be studied by counting completions as a function of current height (Lemma 2.1).*

Completion multiplicity and future-cone entropy. Fix a Dyck prefix u of length k and height h. For a target tier n with $2n \geq k$, define the completion multiplicity

$$M_n(u) := \#\{w \in \mathcal{D}_n : u \preceq w\},$$

the number of completed histories at tier n consistent with the partial history u. This is the finite-tier size of the local cone rooted at u. It depends only on the remaining step budget $r := 2n - k$ and the current height h, and admits the explicit ballot-number formula of Lemma 2.1. The associated future-cone entropy is

$$S_n^{\mathrm{cone}}(u) := \log M_n(u).$$

Information rate as rate of possibility reduction. Let m denote the number of selection events (local contractions) along a history, and let computational proper time be $\tau = \tau_0 m$ for a fixed scale $\tau_0 > 0$. We define the information rate associated with outcome x to be the information loss per unit computational proper time,

$$R(x) := \frac{\Delta S(x)}{\tau}.$$

In the simplest case of a single event ($m = 1$), this reduces to $R(x) = \Delta S(x)/\tau_0$. One may also adopt a coarser tier-wise selection model in which m is identified with the tier index n (one selection per tier boundary), but we keep these notions separate in general.

Gauge-invariant counting. When histories admit a redundancy under commuting spacelike-separated updates, one may quotient the fine-grained history set at tier n by the induced gauge equivalence relation $\sim_g$ of Definition 5.1. When $\mathcal{D}_n$ is taken to parametrize such fine-grained histories at tier n, define $\bar{\mathcal{D}}_n := \mathcal{D}_n/\sim_g$. If f is gauge-invariant (constant on $\sim_g$-orbits), define

$$\bar{N}(x) := \#\{[w] \in \bar{\mathcal{D}}_n : f(w) = x\}, \qquad \bar{\Delta} S(x) := \log\Big(\frac{\#(\bar{\mathcal{D}}_n)}{\bar{N}(x)}\Big),$$

and use $\bar{\Delta} S$ in place of ΔS. This removes overcounting due solely to reordering of independent collapses.

D.2 Size bookkeeping for subtree-selection collapses

In addition to ensemble-level multiplicities, some collapse rules admit a simple size bookkeeping at the level of individual trees. Let T be a finite full binary tree. Define its *internal size* $U(T)$ (number of internal nodes) recursively by

$$U(()) := 0, \qquad U(\bullet(L, R)) := 1 + U(L) + U(R),$$

where $()$ denotes a leaf and $\bullet(L, R)$ denotes a binary pair.

Lemma D.1 (Size drop under subtree selection)**.** *Consider the local collapse that replaces a pair $\bullet(L, R)$ by one of its children:*

$$\bullet(L, R) \rightsquigarrow L \qquad or \qquad \bullet(L, R) \rightsquigarrow R.$$

Then the size drop is

$$U(\bullet(L, R)) - U(L) = 1 + U(R), \qquad U(\bullet(L, R)) - U(R) = 1 + U(L).$$

In particular, if the collapse rule keeps the larger child in U (i.e. keeps $\arg\max\{U(L), U(R)\}$), then the drop is $1 + \min\{U(L), U(R)\}$.

Proof. Immediate from the defining recursion $U(\bullet(L, R)) = 1 + U(L) + U(R)$. $\square$

D.3 Fields on words, prefixes, and nodes (optional)

We use the word "field" as shorthand for a complex-valued function on one of the Catalan objects already in play. Several closely related state spaces are useful in different contexts.

Fields on completed histories (fixed tier). Fix n and consider a function $\Phi_n : \mathcal{D}_n \to \mathbb{C}$ assigning an amplitude (or observable value) to each completed history $w \in \mathcal{D}_n$. The associated Hilbert space is $\ell^2(\mathcal{D}_n)$ with inner product

$$\langle \psi, \phi \rangle := \sum_{w \in \mathcal{D}_n} \overline{\psi(w)}\, \phi(w).$$

Fields on prefixes (the full cone). Let $\mathcal{P}$ denote the set of Dyck prefixes (admissible partial histories). A prefix field is a function $\Phi : \mathcal{P} \to \mathbb{C}$, which may be restricted to a fixed length (tier) slice $\mathcal{P}_k := \{p \in \mathcal{P} : |p| = k\}$ when needed.

Fields on nodes of a fixed tree. Given $w \in \mathcal{D}_n$, let $T(w)$ be its associated full binary tree. A node field is a function $\phi_w : \text{Int}(T(w)) \to \mathbb{C}$ on the internal nodes of that tree.

Remark D.2. *These notions live on different objects (tiers, the prefix poset, or a single tree) and are independent of any within-tier ordering convention on $\mathcal{D}_n$.*

D.4 Subtree indicators as a multiscale spanning family (optional)

Let T be a finite rooted tree and write $\mathrm{Int}(T)$ for its internal nodes. Each $v \in \mathrm{Int}(T)$ determines a rooted subtree T_v, and hence a subset $\mathrm{Int}(T_v) \subseteq \mathrm{Int}(T)$. Define the subtree indicator

$$\chi_v : \mathrm{Int}(T) \to \{0, 1\}, \qquad \chi_v(u) := \mathbf{1}\{u \in \mathrm{Int}(T_v)\}.$$

Lemma D.2 (Subtree indicators form a basis). *The family $\{\chi_v : v \in \mathrm{Int}(T)\}$ is a basis of the vector space of complex-valued functions on $\mathrm{Int}(T)$.*

Proof. Order the internal nodes by nonincreasing depth (deepest first), and let M be the square matrix with entries $M_{uv} := \chi_v(u)$. Then $M_{vv} = 1$ for all v, while $M_{uv} = 0$ whenever u precedes v in this order (a node cannot be a descendant of a deeper node). Thus M is triangular with ones on the diagonal, hence invertible. Therefore the indicators are linearly independent and, since their number equals $\#\mathrm{Int}(T)$, they form a basis. $\square$

Corollary D.1 (Explicit inversion). *Let $f : \mathrm{Int}(T) \to \mathbb{C}$ be any function. There is a unique family of coefficients $\{a_v\}_{v \in \mathrm{Int}(T)}$ such that*

$$f = \sum_{v \in \mathrm{Int}(T)} a_v \chi_v.$$

Writing $\mathrm{par}(v)$ for the parent of v (for $v \neq \mathrm{root}(T)$), these coefficients are given by

$$a_{\mathrm{root}(T)} = f(\mathrm{root}(T)), \qquad a_v = f(v) - f(\mathrm{par}(v)) \quad (v \neq \mathrm{root}(T)).$$

Proof. For each $u \in \mathrm{Int}(T)$, $(\sum_v a_v \chi_v)(u) = \sum_{v:\, u \in \mathrm{Int}(T_v)} a_v = \sum_{v \preceq u} a_v$, where $v \preceq u$ means that v is an ancestor of u. With the stated choice of coefficients, this ancestor sum telescopes along the unique root-to-u chain to yield $f(u)$. Uniqueness follows from Lemma D.2. $\square$

Remark D.3. *This basis is "multiscale": indicators of deep subtrees localize to fine regions of T, while indicators near the root encode coarse structure. Any choice of orthonormalization yields an orthonormal basis adapted to the rooted tree geometry.*

D.5 Operators on a fixed history tree (optional)

In addition to tier-wise state spaces (fields on $\mathcal{D}_n$), one may also consider dynamics *within* a fixed realized history by placing operators on the internal nodes of its tree.

Node Hilbert space. Fix $w \in \mathcal{D}_n$ and let $T(w)$ be its associated full binary tree. Write $V_w := \mathrm{Int}(T(w))$ and consider $\ell^2(V_w)$ with inner product $\langle \psi, \phi \rangle := \sum_{v \in V_w} \overline{\psi(v)}\, \phi(v)$.

Adjacency and Laplacian. Let $G_w = (V_w, E_w)$ be any finite undirected graph on V_w (for example, connect each internal node to its internal children). Define A_{G_w}, D_{G_w}, and the graph Laplacian and generator by

$$\Delta_{G_w} := D_{G_w} - A_{G_w}, \qquad L_{G_w} := -\Delta_{G_w}.$$

Heat and Schrödinger evolutions. The corresponding "internal-time" heat equation is

$$\partial_\tau u = L_{G_w} u,$$

and the corresponding unitary Schrödinger evolution is

$$i\,\partial_t \psi = -L_{G_w}\psi = \Delta_{G_w}\psi.$$

Remark D.4. *This within-history operator framework is independent of the tier-growth Markov dynamics and of coherent summation over histories: it simply records that, once a graph structure is specified on the internal nodes of a fixed Catalan tree, standard graph-Laplacian constructions yield discrete diffusion and Schrödinger-type evolutions on that fixed combinatorial background.*

D.6   Operators on tier slices (optional)

The main text emphasizes two dynamics on the Catalan substrate: tier growth (prefix extension) and coherent summation over histories. Independently, one may also consider *slice dynamics* on a fixed tier by endowing the finite set $\mathcal{D}_n$ with an auxiliary adjacency graph. This subsection records the standard operator framework for such constructions.

Tier Hilbert space. We take the tier state space to be $\ell^2(\mathcal{D}_n)$ as in Section D.3.

Adjacency graphs. Let $G_n = (\mathcal{D}_n, E_n)$ be any finite undirected graph on $\mathcal{D}_n$. The choice of G_n is additional structure: different graphs induce different notions of locality on the tier. A canonical example is the rotation graph (the associahedron adjacency) on full binary trees, where edges correspond to single associativity rotations [20].

Associahedra and planar tree amplitudes (scattering-amplitude tie-in). The associahedron adjacency on $\mathcal{D}_n$ is also natural from the perspective of scattering amplitudes. For the planar tree-level sector of bi-adjoint cubic scalar theory (ϕ^3), Arkani-Hamed, Bai, He, and Yan identify an associahedron in planar kinematic space and show that the tree amplitude is the corresponding canonical form of this positive geometry [18]. From this viewpoint, the Catalan enumeration of planar cubic tree diagrams is not merely counting: the associahedron organizes factorization channels geometrically, and different triangulations correspond to different diagrammatic expansions of the same canonical form (see, e.g., the review [21]). For quartic interactions, an analogous positive-geometry description involves Stokes polytopes rather than associahedra [19].

Tamari/Dyck/alt-Tamari choices on the same tier. The point of introducing an auxiliary graph G_n is that the underlying state set $\mathcal{D}_n$ supports multiple natural notions of tier-locality coming from classical Catalan posets. The rotation graph is the undirected adjacency underlying the Tamari order; one may likewise equip $\mathcal{D}_n$ with adjacency induced by the Dyck ("Stanley") lattice on Dyck paths, or more generally by the family of δ-Tamari (alt-Tamari) posets interpolating between these extremes. These alternatives use different covering relations on the same Catalan tier and therefore induce different graph Laplacians Δ_{G_n} and different "free" tier Hamiltonians, but they live on a common configuration space $\mathcal{D}_n$ [16, 20].

Linear intervals as "1D corridors" in Catalan posets. A useful robustness fact is that certain one-dimensional substructures are invariant across these Catalan posets: Chenevière proves that, for each fixed n and each height parameter k (in the sense of [20]), the Tamari lattice and the Dyck lattice have the same number of *linear intervals* (intervals whose Hasse diagram is a chain), and moreover all alt-Tamari posets share this same count at each height [20]. In the present language, this says that the number of "diamond-free corridors" (regions with a unique maximal chain) is stable under a wide class of tier-local adjacency choices, reinforcing the theme that many distinct dynamics can be layered on a single Catalan substrate without changing its most rigid combinatorial invariants.

Adjacency and Laplacian. Define the adjacency operator A_{G_n} and the degree operator D_{G_n} on $\ell^2(\mathcal{D}_n)$ by

$$(A_{G_n}\psi)(w) := \sum_{w' \sim w} \psi(w'), \qquad (D_{G_n}\psi)(w) := \deg(w)\,\psi(w),$$

where $w' \sim w$ denotes adjacency in G_n. The (combinatorial) graph Laplacian is

$$\Delta_{G_n} := D_{G_n} - A_{G_n},$$

and the associated diffusion generator is

$$L_{G_n} := -\Delta_{G_n}.$$

Then Δ_{G_n} is self-adjoint and positive semidefinite, while L_{G_n} is self-adjoint and negative semidefinite.

Discrete heat and Schrödinger equations. The heat equation on the tier graph is the linear ODE

$$\partial_\tau u = L_{G_n} u,$$

with solution $u(\tau) = e^{\tau L_{G_n}} u(0)$. Because $-\Delta_{G_n}$ is self-adjoint and nonpositive, $e^{\tau L_{G_n}}$ is a contraction semigroup. The corresponding unitary "free" Schrödinger evolution is

$$i\,\partial_t \psi = -L_{G_n}\psi = \Delta_{G_n}\psi,$$

with solution $\psi(t) = e^{-it\Delta_{G_n}}\psi(0)$.

Remark D.5. *This optional tier-graph framework does not fix a preferred choice of adjacency G_n and is not used elsewhere in the paper. Its purpose is to make explicit that, once a tier-local notion of neighbourhood is specified, discrete diffusion and Schrödinger-type evolutions on the Catalan state space follow by standard graph-Laplacian constructions (compare Remark C.5 and Remark C.6 for the tier-growth Markov structure induced by Dyck conditioning).*

E   A Double-Slit Thought Experiment on the Catalan Light Cone

This appendix provides an illustrative thought experiment showing how the discrete path-integral formalism developed in Section 4 exhibits interference in a setting analogous to the double-slit experiment. The construction is entirely combinatorial and finite. No new assumptions, dynamical rules, or continuum limits are introduced; the purpose is solely to instantiate the formalism in a familiar narrative. Throughout, we take the phase functional to be the Dyck area $A(w)$ introduced in Section 4, i.e. $\psi(w) = e^{i\alpha A(w)}$ (a special case of Proposition 4.1).

E.1 Two sources as boundary-conditioned cones

Consider two distinct Dyck prefixes u_L and u_R of equal length and height. Each prefix induces a local Catalan cone of admissible continuations, as described in Section 2.9. We refer to these as the left and right source cones, although no spatial interpretation is assumed at this stage.

Both cones are evolved to a common tier n, producing two ensembles of Dyck paths of semilength n that differ only in their initial boundary condition. The admissible histories from both cones are evaluated relative to the same observable defined below.

E.2 Observable and indistinguishability

Fix a tier n and define an observable

$$f : \mathcal{D}_n \to \mathcal{X},$$

where $\mathcal{X}$ is a discrete outcome space. The observable f retains a coarse-grained feature of each history (for example, a bin determined by the mean height or total area) and discards all other information, including which source cone the history originated from.

Interference arises precisely because histories originating from distinct cones may be rendered indistinguishable by the observable. If the observable were to retain source information, no interference would occur.

E.3 A worked finite example

Take $n = 4$ and choose two admissible Dyck prefixes of equal length and height,

$$u_L = (()\,(, \qquad u_R = ()\,((,$$

each of length 4 and height 2. Each prefix admits exactly three completions to a full Dyck word of length 8, yielding six histories in the union of the two source cones.

Define a coarse observable that discards source information by sampling the height at a fixed time step after the "slits":

$$f(w) := H_w(6) \in \{0, 2\}.$$

This is a discrete analogue of recording transverse displacement at a detector time without access to which slit was taken.

cone	w	$A(w)$	$f(w) = H_w(6)$
L	$(()\,(()))$	12	2
L	$(()\,()\,())$	10	2
L	$(()\,())\,()$	8	0
R	$()\,((()))$	10	2
R	$()\,(()\,())$	8	2
R	$()\,(())\,()$	6	0

Table 1: Two equal-height source cones at $n = 4$ and a coarse detector observable.

With phase $\psi(w) = e^{i\alpha A(w)}$, the detector amplitudes are

$$\Psi(2) = \sum_{f(w)=2} e^{i\alpha A(w)} = e^{i12\alpha} + 2e^{i10\alpha} + e^{i8\alpha} = 2e^{i10\alpha}\big(1 + \cos(2\alpha)\big),$$

$$\Psi(0) = \sum_{f(w)=0} e^{i\alpha A(w)} = e^{i8\alpha} + e^{i6\alpha} = 2e^{i7\alpha}\cos(\alpha).$$

By counting alone one would predict multiplicities $N(2) = 4$ and $N(0) = 2$. In contrast, the Born-style intensities $|\Psi(x)|^2$ vary with α and can exhibit strong suppression. For example, at $\alpha = \pi/2$ one obtains $\Psi(2) = 0$ (exact destructive interference at the outcome $x = 2$), even though $N(2) = 4$ histories contribute.

This example is intentionally tiny: its purpose is to show, in finite combinatorial terms, how (i) multiple histories per outcome, (ii) an additive phase functional, and (iii) coarse observation together produce interference. Larger n yields richer outcome sets and more intricate cancellation patterns.

E.4 Summary

No wave equation, spatial geometry, or continuum approximation is assumed in this construction. The example simply instantiates the general mechanism of Section 4: complex weights, coherent summation over coarse-grained preimages, and Born-style squaring suffice to produce interference.

F Computational Foundations

This appendix records proof sketches for the computational claims used in the main text, including Proposition 3.1 and the disjoint-commutation property of Lemma F.2. For a lean v1, extended examples and additional formal development are omitted.

Lemma F.1 (Internalizing Symbols as Motifs)**.** *Let Σ be a finite (or countable) alphabet of atomic symbols, and consider finite applicative terms over Σ (binary application with atoms). There is an injective encoding of such labeled application trees into the Catalan family $\mathcal{C}$ of unlabeled full binary trees. One explicit construction fixes two distinct tag trees $A, B \in \mathcal{C}$, assigns each $\sigma \in \Sigma$ a distinct motif $S_\sigma \in \mathcal{C} \setminus \{A, B\}$, and defines*

$$E(\sigma) \;:=\; \bullet(A, S_\sigma), \qquad E(t \cdot u) \;:=\; \bullet\big(B, \bullet(E(t), E(u))\big),$$

where $t \cdot u$ denotes application and $\bullet(\cdot, \cdot)$ denotes binary pairing of subtrees. The left tag distinguishes atoms from applications, so E is recursively decodable and therefore injective.

Proof Sketch (of Proposition 3.1). As described in classical treatments of combinatory logic and the λ-calculus [8, 4], application is a binary operation, and every term therefore possesses a unique representation as a full binary tree: internal nodes encode application, and leaves encode variables, constants, or combinators. This establishes a canonical embedding of programs into $\mathcal{C}$.

Conversely, any full binary tree with labeled leaves may be interpreted as a well-formed program term by reading internal nodes as applications and leaves as atomic symbols, yielding a unique term up to α-equivalence.

Operational semantics are defined via local tree rewrites. A β-redex $(\lambda x.M)\,N$ contracts by replacing the parent application with $M[x := N]$; SKI reductions replace specific subtrees according to fixed patterns. In each case, the output remains a full binary tree, so evaluation never leaves $\mathcal{C}$. Because nondeterministic redex choices correspond to branching in the space of trees, each complete reduction sequence is a path through the Catalan possibility space, completing the correspondence.
□

Lemma F.2 (Commutation of disjoint reductions)**.** *Let T be a full binary tree and consider any local rewrite system whose single-step reductions replace a rooted subtree matching a finite pattern by a new subtree, leaving the rest of T unchanged. Suppose two single-step reductions are applicable at positions p and q whose rooted subtrees are disjoint (neither position lies on the root-to-node path of the other). Let T_p denote the result of applying the reduction at p, and similarly T_q. Then both reductions remain applicable after the other, and they commute:*

$$(T_p)_q \ \equiv \ (T_q)_p.$$

In particular, disjoint reductions form a commuting diamond as in Figure 6.

Proof Sketch. Since p and q lie in disjoint subtrees, contracting at p rewrites only the subtree rooted at p and leaves the subtree rooted at q unchanged. Symmetrically, contracting at q leaves the subtree at p unchanged. Because the two rewrite steps act on disjoint parts of the tree, performing both contractions yields the same result regardless of order. □

References

[1] L. Addario-Berry, L. Devroye, and S. Janson. Sub-Gaussian tail bounds for the width and height of conditioned Galton–Watson trees. *Annals of Probability*, 41(2):1074–1087, 2013.

[2] J. Ambjørn, J. Jurkiewicz, and R. Loll. Dynamically triangulating Lorentzian quantum gravity. *Nuclear Physics B*, 610:347–382, 2001.

[3] J. Ambjørn, A. Görlich, J. Jurkiewicz, and R. Loll. Nonperturbative quantum gravity. *Physics Reports*, 519:127–210, 2012.

[4] H. P. Barendregt. *The Lambda Calculus: Its Syntax and Semantics.* North-Holland, 1984.

[5] L. Bombelli, J. Lee, D. Meyer, and R. D. Sorkin. Space-time as a causal set. *Physical Review Letters*, 59(5):521–524, 1987.

[6] A. Church. A set of postulates for the foundation of logic. *Annals of Mathematics*, 34:839–864, 1933.

[7] T. M. Cover and J. A. Thomas. *Elements of Information Theory.* 2nd edition, John Wiley & Sons, 2006.

[8] H. B. Curry and R. Feys. *Combinatory Logic, Vol. I.* North-Holland, 1958.

[9] R. P. Feynman and A. R. Hibbs. *Quantum Mechanics and Path Integrals.* McGraw–Hill, 1965. (Dover reprint, 2010).

[10] S. Janson. Brownian excursion area, Wright's constants in graph enumeration, and other Brownian areas. *Probability Surveys*, 4:80–145, 2007.

[11] M. Kac. On distributions of certain Wiener functionals. *Transactions of the American Mathematical Society*, 65(1):1–13, 1949.

[12] J.-F. Le Gall. Random trees and applications. *Probability Surveys*, 2:245–311, 2005.

[13] R. Orús. A practical introduction to tensor networks: Matrix product states and projected entangled pair states. *Annals of Physics*, 349:117–158, 2014.

[14] J. Pitman. Brownian motion, bridge, excursion, and meander revisited. *Electronic Journal of Probability*, 4:1–32, 1999.

[15] C. Rovelli. *Quantum Gravity*. Cambridge University Press, 2004.

[16] R. P. Stanley. *Catalan Numbers*. Cambridge University Press, 2015.

[17] L. Takács. A Bernoulli excursion and its various applications. *Advances in Applied Probability*, 23(3):557–585, 1991.

[18] N. Arkani-Hamed, Y. Bai, S. He, and G. Yan. Scattering forms and the positive geometry of kinematics, color and the worldsheet. *JHEP* **05** (2018) 096. arXiv:1711.09102.

[19] P. Banerjee, A. Laddha, and P. Raman. Stokes polytopes: The positive geometry for ϕ^4 interactions. arXiv:1811.05904, 2018.

[20] C. Chenevière. Linear intervals in the Tamari and the Dyck lattices and in the alt-Tamari posets. arXiv:2209.00418v2, 2022.

[21] E. Herrmann and J. Trnka. Positive geometry of scattering amplitudes. arXiv:2203.13018, 2022.